

1 Technical Note: Preventing CO<sub>2</sub> overestimation from mercuric or  
2 copper (II) chloride preservation of dissolved greenhouse gases in  
3 freshwater samples

4

5 François Clayer<sup>1\*</sup>, Jan Erik Thrane<sup>1</sup>, Kuria Ndungu<sup>1</sup>, Andrew King<sup>1</sup>, Peter Dörsch<sup>2</sup>, Thomas Rohrlack<sup>2</sup>

6

7 <sup>1</sup>Norwegian Institute for Water Research (NIVA), Økernveien 94, 0579 Oslo, Norway

8

9 <sup>2</sup>Faculty of Environmental Sciences and Natural Resource Management, Norwegian University of  
10 Life Sciences, PO Box 5003, 1432 Ås, Norway

11

12 \*Corresponding author(s): François Clayer ([francois.clayer@niva.no](mailto:francois.clayer@niva.no))

13

14 **Abstract**

15 The determination of dissolved gases (O<sub>2</sub>, CO<sub>2</sub>, CH<sub>4</sub>, N<sub>2</sub>O, N<sub>2</sub>) in surface waters allows to estimate  
16 biological processes and greenhouse gas fluxes in aquatic ecosystems. Mercuric chloride (HgCl<sub>2</sub>) has  
17 been widely used to preserve water samples prior to gas analysis. However, alternates are needed  
18 because of the environmental impacts and prohibition of mercury. HgCl<sub>2</sub> is a weak acid and interferes  
19 with dissolved organic carbon (DOC). Hence, we tested the effect of HgCl<sub>2</sub> and two substitutes  
20 (copper (II) chloride – CuCl<sub>2</sub> and silver nitrate – AgNO<sub>3</sub>), as well as storage time (24h to 3 months)  
21 on the determination of dissolved gases in low ionic strength and high DOC water from a typical  
22 boreal lake. Furthermore, we investigated and predicted the effect of HgCl<sub>2</sub> on CO<sub>2</sub> concentrations in  
23 periodic samples from another lake experiencing pH variations (5.4–7.3) related to *in situ*  
24 photosynthesis. Samples fixed with inhibitors generally showed negligible O<sub>2</sub> consumption. However,  
25 effective preservation of dissolved CO<sub>2</sub>, CH<sub>4</sub> and N<sub>2</sub>O for up to three months prior to dissolved gas  
26 analysis, was only achieved with AgNO<sub>3</sub>. In contrast, HgCl<sub>2</sub> and CuCl<sub>2</sub> caused an initial increase in  
27 CO<sub>2</sub> and N<sub>2</sub>O from 24h to 3 weeks followed by a decrease from 3 weeks to 3 months. The CO<sub>2</sub>  
28 overestimation, caused by HgCl<sub>2</sub>-acidification and shift in the carbonate equilibrium, can be  
29 calculated from predictions of chemical speciation. Errors due to CO<sub>2</sub> overestimation in HgCl<sub>2</sub>-  
30 preserved water, sampled from low ionic strength and high DOC freshwater that are common in the  
31 northern hemisphere, could lead to an overestimation of the CO<sub>2</sub> diffusion efflux by a factor of >20  
32 over a month, or a factor of 2 over the ice-free season. The use of HgCl<sub>2</sub> and CuCl<sub>2</sub> for freshwater  
33 preservation should therefore be discontinued. Further testing of AgNO<sub>3</sub> preservation should be  
34 performed under a large range of freshwater chemical characteristics.

CO<sub>2</sub> overestimation from HgCl<sub>2</sub> fixation – Clayer et al.

35

36 **Key-words:** lake, greenhouse gases, water sample preservation, mercuric chloride, metal toxicity,  
37 carbon dioxide

38 **Running tile:** CO<sub>2</sub> overestimation from HgCl<sub>2</sub> fixation

## 39 **1 Introduction**

40

41 The determination of dissolved gases by gas chromatography from water samples collected in the  
42 field allows the estimation of biological processes in aquatic ecosystems such as photosynthesis and  
43 oxic respiration (O<sub>2</sub>, CO<sub>2</sub>), denitrification (N<sub>2</sub>, N<sub>2</sub>O) and methanogenesis (CH<sub>4</sub>). This technique is also  
44 useful to test the calibration of *in-situ* sensors in long term deployment. However, the accuracy of this  
45 approach largely depends on the effectiveness of sample fixation. In fact, the partial pressure of the  
46 dissolved gases will continue to evolve in the water sample from the time of collection to the time of  
47 analysis unless biological activity is prevented. This is an issue when field sites are far from  
48 laboratory facilities, and when samples need to be stored until the end of the field season for more  
49 efficient processing in large batches. Hence, before using a given chemical to preserve water samples,  
50 it must be ensured that it is efficient in inhibiting biological activity without changing the sample's  
51 chemistry.

52 Mercuric (II) chloride (HgCl<sub>2</sub>) has been widely used as an inhibitor of the above-mentioned biological  
53 processes to preserve water samples for the determination of dissolved CO<sub>2</sub> in seawaters (e.g.  
54 Dickson, Sabine & Christian, 2007) and several dissolved gases in natural and artificial freshwater  
55 bodies (e.g. O<sub>2</sub>, CO<sub>2</sub>, CH<sub>4</sub>, N<sub>2</sub> and/or N<sub>2</sub>O; Guérin et al., 2006; Hessen et al., 2017; Hilgert et al.,  
56 2019; Okuku et al., 2019; Schubert et al., 2012; Xiao et al., 2014; Yan et al., 2018; Yang et al., 2015)  
57 because it proved effective at very low concentrations compared to other reagents (e.g. Horvatić &  
58 Peršić, 2007; Hassen *et al.*, 1998). Worldwide efforts have sought to reduce the use of mercury  
59 because it is considered toxic to the environment and exposure can severely affect human health  
60 (Chen et al., 2018). Therefore, alternative preservation techniques to HgCl<sub>2</sub> treatment have been tested  
61 for dissolved inorganic carbon (DIC) and δ<sup>13</sup>C-DIC such as acidification with phosphoric acid  
62 (Taipale & Sonninen, 2009) or a combination of filtration and exposure to benzalkonium chloride or  
63 sodium chloride (Takahashi *et al.*, 2019). Previous studies showed that simple filtration (and cooling),  
64 fixation (precipitation) or acidification were effective in preserving water samples (Wilson, Munizzi  
65 & Erhardt, 2020). An alternative to using preservatives is to collect in-situ water samples, extract the  
66 headspace in the field, and analyze the headspace in a laboratory (e.g., Cole et al., 1994; Karlsson et  
67 al., 2013; Kling et al., 1991). However, these techniques were not tested for the simultaneous  
68 determination of several dissolved gases, including CH<sub>4</sub> which is subject to rapid degassing during  
69 handling or storage if samples are not preserved because of its low solubility in water (Duan & Mao,  
70 2006). In addition, some of the existing alternatives, such as filtration or field headspace equilibration,  
71 are difficult to operate in remote areas in the field under harsh weather conditions and prone to  
72 potential ambient air contamination. Solutions for water sample preservation should therefore involve  
73 a minimum of manipulation steps in the field to avoid gas exchange with ambient air. Preservative  
74 amendments into sealed water bottles appears as one of the most efficient methods. Copper(II)

75 chloride (CuCl<sub>2</sub>) and silver nitrate (AgNO<sub>3</sub>), the most toxic form of silver, are relevant alternatives to  
76 HgCl<sub>2</sub> given their known toxicity (e.g., Ratte 2009; Amorim and Scott-Fordsmand 2012) and wide  
77 application in water treatments and water purification (Larrañaga et al., 2016; Nowack et al., 2011;  
78 NPIRS, 2023; Ullmann et al., 1985). Nevertheless, the efficiency of these alternative preservatives has  
79 never been tested for dissolved gas samples preservation.

80 The addition of HgCl<sub>2</sub> to water is known to produce hydrochloric acid through hydrolysis (Ciavatta &  
81 Grimaldi, 1968) and to form complexes with many environmental ligands, both inorganic (Powell *et*  
82 *al.*, 2004) and organic (Tipping, 2007; Foti *et al.*, 2009; Liang *et al.*, 2019; Chen *et al.*, 2017). The  
83 complexation of Hg<sup>+</sup> with the carboxyl or thiol groups of DOC in oxic environments could further  
84 increase the concentration of H<sup>+</sup> (Khwaja et al., 2006; Skyllberg, 2008). This acidification can be an  
85 issue in poorly buffered water (low ionic strength) with high concentration of DOC where a shift in  
86 the pH and carbonate equilibrium can be induced. In that case, the estimated CO<sub>2</sub> concentration would  
87 be higher after HgCl<sub>2</sub> fixation than the *in situ* concentration, and if the shift in pH is not accounted for,  
88 can result in an overestimation of dissolved CO<sub>2</sub> and bicarbonate concentrations. A similar  
89 acidification effect is also expected with CuCl<sub>2</sub> treatments (Rippner et al., 2021), but not for AgNO<sub>3</sub>  
90 treatments. Such effects would not be expected in marine water due to the high ionic strength of the  
91 water (Chou *et al.*, 2016) or freshwater with low pH (<5.5) under which conditions nearly all  
92 dissolved inorganic carbon is CO<sub>2</sub> (Stumm & Morgan, 1981). Thus, there are clear limits of the  
93 application of HgCl<sub>2</sub>, and possibly CuCl<sub>2</sub>, for freshwater sample preservation given its risk of leading  
94 to overestimation of CO<sub>2</sub> and bicarbonate concentrations, in addition to exposing field workers to the  
95 risks of its high toxicity.

96

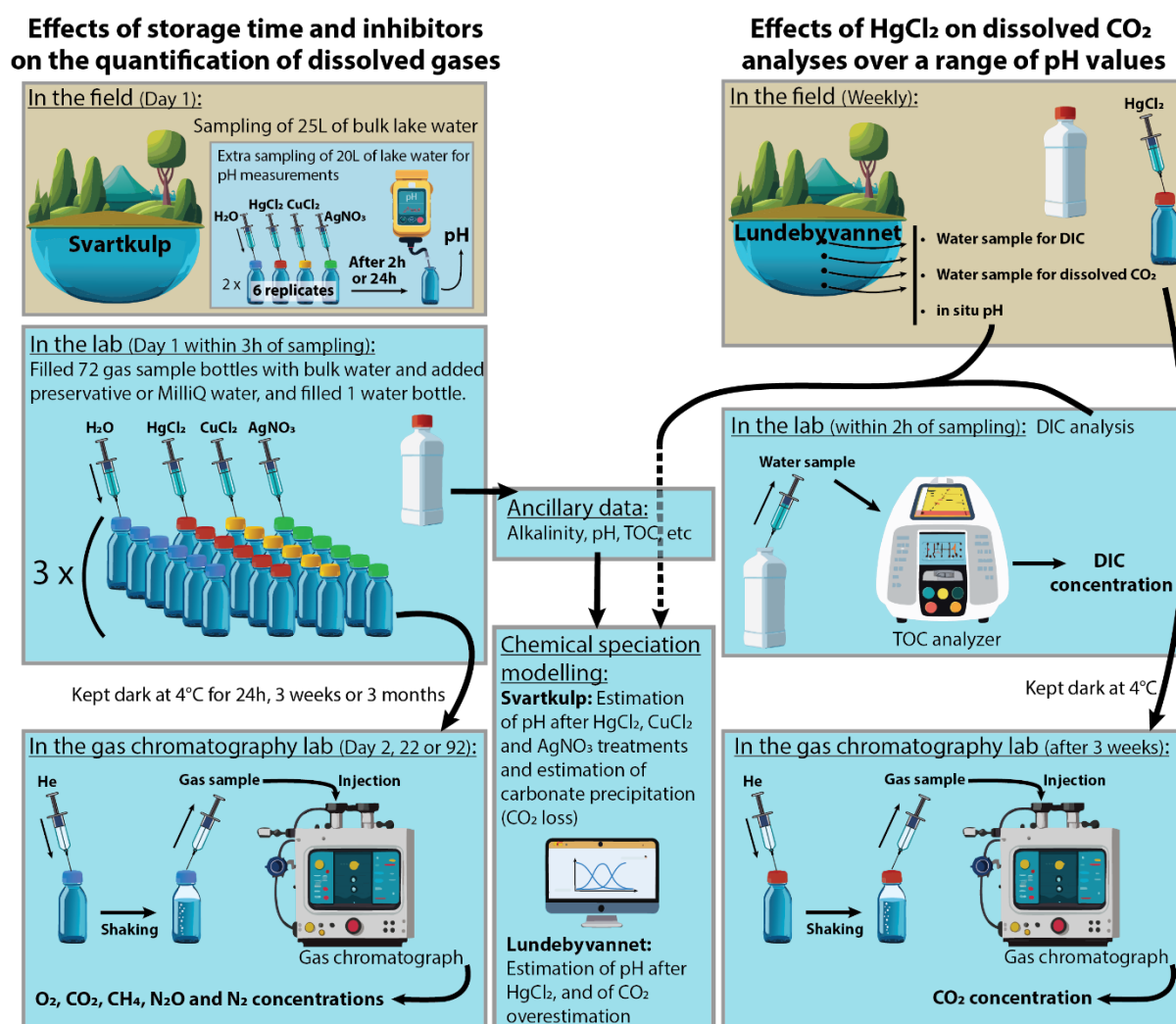
97 Here we combine data from laboratory experiments (i) and field work (ii) to illustrate risks of mis-  
98 estimation of dissolved gas concentrations in freshwaters with some preservatives and provide  
99 recommendation for best practices in the field. First, we (i) performed some short-term and long-term  
100 incubations of water from a typical heterotrophic unproductive boreal lake with circumneutral pH,  
101 low ionic strength (poor buffering capacity) and high DOC concentration to test the effect of storage  
102 time and different preservative treatments on the determination of five dissolved gases (O<sub>2</sub>, CO<sub>2</sub>, CH<sub>4</sub>,  
103 N<sub>2</sub> and N<sub>2</sub>O) by headspace equilibration and gas chromatography. The preservatives were mercuric  
104 chloride (HgCl<sub>2</sub>) and two alternative inhibitors, chosen for their wide and effective application in  
105 water treatments and water purification (copper (II) chloride – CuCl<sub>2</sub> and silver nitrate – AgNO<sub>3</sub>; Xu  
106 & Imlay, 2012; Rai, Gaur & Kumar, 1981). Unamended water samples, where only ultrapure water  
107 was added, were also included for comparison. In addition, we (ii) analysed dissolved CO<sub>2</sub>  
108 concentration data obtained from a typical productive boreal lake using two independent methods, one  
109 by gas chromatography following HgCl<sub>2</sub> fixation, and one through dissolved inorganic carbon

110 determination without fixation. We show that the overestimation of dissolved CO<sub>2</sub> concentrations  
 111 caused by HgCl<sub>2</sub> fixation can be predicted based on chemical equilibria.

112

113 **2. Methods**

114 The detailed experimental procedures for investigating (i) the effects of storage time and different  
 115 inhibitors on dissolved gas concentrations as well as (ii) the effects of HgCl<sub>2</sub> on dissolved CO<sub>2</sub>  
 116 analyses over a range of pH values are summarized in Fig. 1 and described below.



117

118 **Fig. 1.** Overview of experimental procedures. Several graphic items in this figure have been generated  
 119 with the help of Adobe® Firefly™ Artificial Intelligence generator.

120 2.1. Effects of storage time and inhibitors on the quantification of dissolved gases

121 *Study site and sampling*

122 Surface water was collected from Lake Svartkulp (59.9761313 N, 10.7363544 E; Southeast Norway)  
123 north of Oslo, Norway, on the 4<sup>th</sup> of September 2019. A 5 L plastic bottle was gently pushed into the  
124 water and progressively tilted to let the water flow into the bottles without bubbling. The bottle  
125 aperture was covered with a 90 µm plankton net to avoid sampling large particles. This procedure was  
126 repeated five times to yield a total water volume of 25 L. The 5 L water bottles were immediately  
127 brought back to the lab. Upon arrival at the laboratory, after temperature equilibration, water from the  
128 5 L bottles was slowly poured, to limit gas exchange with the ambient air, into a 25 L tank to provide  
129 a single bulk sample to start the incubation experiment. Filtration, e.g., with 0.45 or 0.2 µm filters,  
130 was avoided to minimize changes in dissolved gas concentrations (e.g., Magen et al., 2014). The  
131 mixed water sample (25 L) was sub-sampled (0.5 L) for the determination of alkalinity (127 µmol L<sup>-1</sup>)  
132 <sup>1</sup>), pH (6.73), ammonium (3 µg N L<sup>-1</sup>), nitrate (5 µg N L<sup>-1</sup>), total N (230 µg N L<sup>-1</sup>), phosphate (1 µg P  
133 L<sup>-1</sup>), total P (9 µg P L<sup>-1</sup>) and TOC (8.9 mg C L<sup>-1</sup>) all analysed by standard methods at the accredited  
134 Norwegian Institute for Water Research (NIVA) lab (see Tab. S1). *In situ* temperature of the lake  
135 water was measured with a handheld thermometer and was 18.5 °C. Note that particulate organic  
136 carbon is a negligible fraction of TOC in Norwegian lake waters, representing on average less than  
137 3% (de Wit et al., 2023).

138 Lake Svartkulp was selected for this experiment because it is representative of low ionic strength  
139 Northern Hemisphere lakes, typically found in granitic bedrock regions in North-East America and  
140 Scandinavia. It is a typical low-productivity, heterotrophic, slightly acidic to neutral, moderately  
141 humic lake. Similar lakes are found in Southern Norway (de Wit et al., 2023), large parts of Sweden  
142 (Valina et al. 2014), Finland, Atlantic Canada (Houle et al., 2022), Ontario, Québec, and North-East  
143 USA (Skjelkvåle and de Wit 2011; Weyhenmeyer et al., 2019).

#### 144 *Laboratory incubation experiment with different preservatives and storage times*

145 The experimental design involved to incubate 72 borosilicate glass bottles (120 mL) filled with lake  
146 water from our 25 L bulk sample subjected to four different treatments: addition of 240 µL of a  
147 preservative solution of (i) HgCl<sub>2</sub>, (ii) CuCl<sub>2</sub> or a (iii) AgNO<sub>3</sub>, or addition of 240 µL of (iv) MilliQ  
148 water. The bottles amended with MilliQ water are hereafter referred to as “unfixed”. The 72 bottles  
149 were divided into three groups which were incubated cold (+4°C) and dark for 24h, three weeks or  
150 three months respectively, before being processed for dissolved gas analysis by gas chromatography.  
151 These incubation times were selected to represent situations where samples are processed directly  
152 upon return to the laboratory (24h), or after medium (3 weeks) to long (3 months) -term storage,  
153 respectively. At each time point and for each treatment, a group of 6 bottles were further processed for  
154 dissolved gas analysis. Concentrations of O<sub>2</sub>, N<sub>2</sub>, N<sub>2</sub>O, CO<sub>2</sub> and CH<sub>4</sub> were determined by gas  
155 chromatography (see below) using the headspace technique following Yang *et al.* (2015). pH was not  
156 measured at the end of the storage period.

157 In details, within 3h of lake water sampling, the 120mL bottles were gently filled with water from the  
 158 mixed sample (25 L). Each 120mL bottle was slowly lowered into the water and progressively tilted  
 159 to let the water flow into the bottle without bubbling. The bottle was then capped under water with a  
 160 gas tight butyl rubber stopper after ensuring that there were no air bubbles in the bottle. The bottles  
 161 were randomized prior to preservative or MilliQ treatment. The preservative or MilliQ amendment  
 162 was pushed in each bottle with a syringe and needle through the rubber septum. To avoid  
 163 overpressure, another needle was placed through septum at the same time, at least 2 cm above the  
 164 other needle, to allow an equivalent volume of clean water to be released.

165 Stock solutions of HgCl<sub>2</sub>, CuCl<sub>2</sub> and AgNO<sub>3</sub> were prepared according to Tab. 1 using high accuracy  
 166 chemical equipment (e.g., high accuracy scale, volumetric flasks). The Ag (Silver nitrate EMSURE®  
 167 ACS; Merck KGaA, Germany) Cu (Copper(II) chloride dihydrate; Merck Life Science ApS, Norway)  
 168 and Hg (Mercury(II) chloride; undetermined) salts were dissolved in MilliQ ultrapure water (>18 MΩ  
 169 cm). For measurement of CO<sub>2</sub> in seawater samples, the standard method involves poisoning the  
 170 samples by adding a saturated HgCl<sub>2</sub> solution in a volume equal to 0.05-0.02% of the total volume  
 171 (Dickson 2007). We used this as a starting point and added 0.02 % saturated HgCl<sub>2</sub> solution to 18  
 172 bottles (240 μL of HgCl<sub>2</sub> 10× diluted saturated solution), resulting in a sample concentration of 14 μg  
 173 HgCl<sub>2</sub> mL<sup>-1</sup> (51.6 μM; Tab. 1). Based on estimated toxicity relative to Hg (Deheyn et al., 2004; Halmi  
 174 et al., 2019), the silver and copper salts were added in molar concentrations equal to two and three  
 175 times the molar concentration of HgCl<sub>2</sub>, respectively (Tab. 1), although it varies between species of  
 176 microorganisms and environmental matrices (Hassen *et al.*, 1998; Rai, Gaur & Kumar, 1981).

177 **Tab. 1.** Stock and sample concentrations of HgCl<sub>2</sub>, CuCl<sub>2</sub> and AgNO<sub>3</sub>.

Salt	Stock solution	Sample concentration	Rationale
HgCl <sub>2</sub>	70 g/L (saturated)	14.0±0.01 μg/mL (51.6 μM)	Dickson, Sabine & Christian, 2007
CuCl <sub>2</sub>	131.9 g/L	26.4±0.02 μg/mL (154.7 μM)	3 × Hg
AgNO <sub>3</sub>	87.6 g/L	17.5±0.02 μg/mL (103.1 μM)	2 × Hg

178

179 *Additional 24h incubation experiment with different preservatives for pH measurements*

180 Since pH was not measured at the end of the first incubation experiment, we performed an additional  
 181 experiment to document any potential rapid (within 24h) impacts of preservative on pH. A total of 48  
 182 borosilicate glass bottles (120 mL) filled with lake water were subjected to the same four different  
 183 treatments as the first experiment described above: HgCl<sub>2</sub>, CuCl<sub>2</sub>, AgNO<sub>3</sub> or MilliQ water  
 184 amendments. To this end, a 20L water tank was filled with surface water from Lake Svartkulp on the  
 185 14<sup>th</sup> of December 2023. The water tank was immediately returned to the laboratory and left for 24h  
 186 equilibrate to the room temperature. On December 15<sup>th</sup>, 120mL bottles were gently filled with water

187 from the bulk 20L sample, as described above. The bottles were randomized prior to preservative or  
188 MilliQ treatment performed as described above. The bottles were then incubated at room temperature  
189 for 2h or 24h. pH was measured in the initial unamended lake water, in 24 bottles opened after 2h  
190 incubation, and in 24 bottles opened after 24h incubation. pH measurements were performed with a  
191 WTW Multi 3620 pH meter calibrated using a two-point calibration at pH = 4 and pH = 7. All pH  
192 measures were corrected for temperature. Water temperature of the water samples during pH  
193 measurements ranged between 19.1 and 21.2°C.

194

## 195 2.2. Effects of HgCl<sub>2</sub> on dissolved CO<sub>2</sub> analyses over a range of pH values

### 196 *Study site and sampling*

197 Water samples were collected from Lake Lundebyvannet located southeast of Oslo (59.54911 N,  
198 11.47843 E, Southeast Norway). Two sets of samples were taken from 1, 1.5, 2 and 2.5 m depth  
199 using a water sampler once or twice a week between April 2020 and January 2021 for the  
200 determination of (i) dissolved CO<sub>2</sub> by GC analysis following fixation with HgCl<sub>2</sub> and (ii) DIC  
201 analysis with a TOC analyser. Samples for GC analysis were filled into 120 mL glass bottles (as  
202 described above for the 72 incubation bottles), which were sealed with rubber septa under water  
203 without air bubbles. Samples for GC analysis were preserved in the field by adding a half-saturated (at  
204 20°C) solution of HgCl<sub>2</sub> (150 µL) through the rubber seal of each bottle using a syringe, as described  
205 above the 72 incubation bottles, resulting in a concentration of 161 µM similar to previous studies  
206 (Clayer et al., 2021; Hessen et al., 2017; Yang et al., 2015). Samples for DIC analysis were filled  
207 without bubbles in 100 ml Winkler glass bottles that were sealed airtight directly after sampling.  
208 These samples were not fixed in any way and were analysed by a TOC analyzer within two hours.  
209 Note that estimation of dissolved CO<sub>2</sub> concentrations from pH and DIC is the least uncertain method  
210 of indirect CO<sub>2</sub> concentration with estimated relative error of 6% or less (Golub et al., 2017). Lake  
211 water temperature and pH were measured *in-situ* using HOBO pH data loggers placed at 1, 1.5, 2 and  
212 2.5 m (Elit, Gjerdrum, Norway).

213 Lake Lundebyvannet has a surface area of 0.4 km<sup>2</sup> and a maximum depth of 5.5 m. It often  
214 experiences large blooms of *G. semen* over the summer between May and September (Hagman et al.,  
215 2015; Rohrlack, 2020). The lake water is characterised by high and fluctuating concentrations of  
216 humic substances (with DOC concentrations ranging from 8 to 28 mg C L<sup>-1</sup>), ammonium (5 to 100 µg  
217 N L<sup>-1</sup>), nitrate (20 to 700 µg N L<sup>-1</sup>), total N (average of 612 µg N L<sup>-1</sup>), phosphate (2 to 4 µg P L<sup>-1</sup>),  
218 total P (average of 28 µg P L<sup>-1</sup>; Rohrlack et al., 2020; Hagman et al., 2015), a fluctuating pH (from 5.5  
219 to 7.3), weak ionic strength with alkalinity ranging between 30 and 150 µmol L<sup>-1</sup>, and electric  
220 conductivity varying from 40 to 70 µS cm<sup>-1</sup>. For more details, see Rohrlack *et al.* (2020).



221 Lake Lundebyvannet was selected for this experiment because it is representative of productive, low-  
222 ionic strength Northern Hemisphere lakes typically found in the southern part of granitic bedrock  
223 regions in North-East America and Scandinavia.

### 224 2.3. Analytical chemistry

#### 225 *Gas chromatography*

226 Headspace was prepared by gently backfilling sample bottles with 20–30 mL helium (He; 99,9999%)  
227 into the closed bottle while removing a corresponding volume of water. Care was taken to control the  
228 headspace pressure within 5% of ambient and a slight He overpressure was released before  
229 equilibration. The bottles were shaken horizontally at 150 rpm for 1 h to equilibrate gases between  
230 sample and headspace. The temperature during shaking was recorded by a data logger. Immediately  
231 after shaking, the bottles were placed in an autosampler (GC-Pal, CTC, Switzerland) coupled to a gas  
232 chromatograph (GC) with He back-flushing (Model 7890A, Agilent, Santa Clara, CA, US).

233 Headspace gas was sampled (approx. 2 mL) by a hypodermic needle connected to a peristaltic pump  
234 (Gilson Minipuls 3), which connected the autosampler with the 250 µL heated sampling loop of the  
235 GC.

236 The GC was equipped with a 20-m wide-bore (0.53 mm) Poraplot Q column for separation of CH<sub>4</sub>,  
237 CO<sub>2</sub> and N<sub>2</sub>O and a 60 m wide-bore Molsieve 5Å PLOT column for separation of O<sub>2</sub> and N<sub>2</sub>, both  
238 operated at 38°C and with He as carrier gas. N<sub>2</sub>O and CH<sub>4</sub> were measured with an electron capture  
239 detector run at 375°C with Ar/CH<sub>4</sub> (80/20) as makeup gas, and a flame ionization detector,  
240 respectively. CO<sub>2</sub>, O<sub>2</sub>, and N<sub>2</sub> were measured with a thermal conductivity detector (TCD). Certified  
241 standards of CO<sub>2</sub>, N<sub>2</sub>O, and CH<sub>4</sub> in He were used for calibration (AGA, Germany), whereas air was  
242 used for calibrating O<sub>2</sub> and N<sub>2</sub>. The analytical error for all gases was lower than 2%. For the Lake  
243 Lundebyvannet time series, CO<sub>2</sub> was separated from other gases using the 20 m wide-bore (0.53 mm)  
244 Poraplot Q column while the other gases were not measured.

245 The results from gas chromatography give the relative concentration of dissolved gases (in ppm) in  
246 the headspace in equilibrium with the water. For the lab experiment with Svartkulp samples (section  
247 2.1), the concentration of dissolved gases in the water at equilibrium with the headspace were  
248 calculated from the temperature corrected Henry constant in water using Carroll, Slupsky and Mather  
249 (1991) for CO<sub>2</sub>, Weiss and Price (1980) for N<sub>2</sub>O, Yamamoto, Alcauskas and Crozier (1976) for CH<sub>4</sub>,  
250 Millero, Huang and Laferiere (2002) for O<sub>2</sub>, Hamme and Emerson (2004) for N<sub>2</sub>. For the Lake  
251 Lundebyvannet time series (section 2.2), the concentration of CO<sub>2</sub> in the water samples were  
252 determined using temperature-dependent Henry's law constants given by Wilhelm, Battino and  
253 Wilcock (1977). The quantities of gases in the headspace and water were summed to find the  
254 concentrations and partial pressures of dissolved gases from the water collected in the field as follows:

$$[gas] = \frac{p_{gas}HV_{water} + \frac{p_{gas}V_{headspace}}{RT}}{V_{water}} \quad (\text{Eq. 1})$$

where [gas] is the gas aqueous concentration,  $p_{gas}$  is the gas partial pressure,  $H$  is the Henry constant,  $V_{water}$  is the volume of water sample during headspace equilibration,  $V_{headspace}$  is the headspace gas volume during equilibration,  $R$  is the gas constant and  $T$  the temperature during headspace equilibration (recorded during shaking). The calculations were similar to Yang *et al.* (2015).

#### DIC analyses

DIC analysis was performed for the Lake Lundebyvannet time series using a Shimadzu TOC-V CPN (Oslo, Norway) instrument equipped with a non-dispersive infrared (NDIR) detector with O<sub>2</sub> as a carrier gas at a flow rate of 100 mL min<sup>-1</sup>. Two to three replicate measurements were run per sample. The system was calibrated using a freshly prepared solution containing different concentrations of NaHCO<sub>3</sub> and Na<sub>2</sub>CO<sub>3</sub> and standards were measured in between each 6<sup>th</sup> sample. CO<sub>2</sub> concentrations in water samples ([CO<sub>2</sub>]) were calculated on the bases of temperature, pH and DIC concentrations as follows (Rohrlack *et al.*, 2020):

$$[CO_2] = \frac{[H^+]^2 C_T}{Z} \quad (\text{Eq. 2})$$

where  $[H^+]$  is the proton concentration ( $10^{-pH}$ ),  $C_T$  is the dissolved inorganic carbon concentration and  $Z$  is given by:

$$Z = [H^+]^2 + K_1[H^+] + K_1K_2 \quad (\text{Eq. 3})$$

where  $K_1$  and  $K_2$  are the first and second carbonic acid dissociation constant adjusted for temperature ( $pK_1 = 6.41$  and  $pK_2 = 10.33$  at 25°C; Stumm & Morgan, 1996).

#### 2.4. Data analysis

##### *pCO<sub>2</sub> and saturation deficit*

Lake Lundebyvannet CO<sub>2</sub> concentrations provided by GC and DIC analyses were converted to pCO<sub>2</sub> (in μatm) as follows:

$$pCO_2 = \frac{[CO_2]}{0.987 \times K_H P_{atm}} \quad (\text{Eq. 4})$$

where  $K_H$  is Henry constant for CO<sub>2</sub> adjusted for in-situ water temperature (Stumm & Morgan, 1996) and  $P_{atm}$  is the atmospheric pressure in bar approximated by:

$$283 \quad P_{atm} = (1013 - 0.1 \times altitude) \times 0.001 \quad (\text{Eq. 5})$$

284 where *altitude* is the altitude above sea level of Lake Lundebyvannet (158 m). Finally, the CO<sub>2</sub>  
285 saturation deficit ( $Sat_{CO_2}$  in  $\mu\text{atm}$ ) was given by

$$286 \quad Sat_{CO_2} = pCO_2 - [CO_2]_{air} \quad (\text{Eq. 6})$$

287 where  $[CO_2]_{air}$  is the pCO<sub>2</sub> in the air (416  $\mu\text{atm}$  for 2020 in Southern Norway retrieved from EBAS  
288 database; NILU, 2022; Tørseth et al., 2012).  $Sat_{CO_2}$  gives the direction of CO<sub>2</sub> flux at the water-  
289 atmosphere interface, and its product with gas transfer velocity determine the CO<sub>2</sub> flux at the water-  
290 atmosphere interface, i.e., whether lake ecosystems are sink ( $Sat_{CO_2} < 0$ ) or source ( $Sat_{CO_2} > 0$ ) of  
291 atmospheric CO<sub>2</sub>.

292

### 293 *Statistical analyses*

294 The effect of storage time and treatment on five dissolved gases (O<sub>2</sub>, N<sub>2</sub>, CO<sub>2</sub>, CH<sub>4</sub>, N<sub>2</sub>O) from the  
295 Lake Svartkulp samples was tested with a two-way ANOVA at an alpha level adapted using the  
296 Bonferroni correction for multiple testing, i.e.,  $\alpha=0.05/5=0.01$ . To evaluate the impact of Hg fixation  
297 on Lake Lundebyvannet samples,  $[CO_2]$  values determined by headspace equilibration and GC  
298 analysis of HgCl<sub>2</sub>-fixed samples were compared with those calculated from DIC measurements of  
299 unfixed samples with a paired t-test.

300 A regression analysis was performed to describe the overestimation of CO<sub>2</sub> concentrations caused by  
301 HgCl<sub>2</sub> fixation in Lake Lundebyvannet samples as a function of pH. The total CO<sub>2</sub> concentration in  
302 the HgCl<sub>2</sub>-fixed samples ( $[CO_2]_{HgCl_2}$ ) can be expressed as:

$$303 \quad [CO_2]_{HgCl_2} = [CO_2]_i + [CO_2]_{ex} \quad (\text{Eq. 7})$$

304 where  $[CO_2]_i$  is the initial CO<sub>2</sub> concentration prior to HgCl<sub>2</sub> fixation, i.e., CO<sub>2</sub> concentration in the  
305 unfixed samples, and  $[CO_2]_{ex}$  is the excess CO<sub>2</sub> concentration caused by a decrease in pH following  
306 HgCl<sub>2</sub> fixation. The relative CO<sub>2</sub> overestimation ( $E$  in %) is given by:

$$307 \quad E = \frac{[CO_2]_{HgCl_2} - [CO_2]_i}{[CO_2]_i} = \frac{[CO_2]_{ex}}{[CO_2]_i} \quad (\text{Eq. 8})$$

308 The impact of pH (or  $[H^+]$ ) on  $E$  was mathematically described by running a regression analysis  
309 using MATLAB®. The *fminsearch* MATLAB function from the Optimization toolbox was used to  
310 find the minimum sum of squared residuals (SSR) for functions of the form of:  $E = A/[H^+]$  or  $E =$   
311  $A \times 10^{-B \times pH}$ . For each optimal solution, the root-mean-square error (RMSE) and coefficient of  
312 determination ( $R^2$ ) were calculated against observed values of  $E$ , i.e., values of  $E$  determined  
313 empirically from observed  $[CO_2]_i$  and  $[CO_2]_{ex}$ .

314

315 *Chemical speciation, saturation-index calculations, and prediction of CO<sub>2</sub> overestimation*

316 The speciation of solutes and saturation index values (SI) of selected minerals were calculated with  
317 the program PHREEQC developed by the USGS (Parkhurst & Appelo, 2013), neglecting the effect of  
318 dissolved organic matter. This was used to assess the impact of the addition of preservative on pH and  
319 shifting the carbonate equilibrium as well as dissolved inorganic carbon losses due to carbonate  
320 mineral precipitation. PHREEQC is commonly used to calculate the speciation of inorganic carbon,  
321 the SI of carbonate minerals and to help estimate the fate of inorganic carbon in carbon cycling  
322 studies (Atekwana et al. 2016; Clayer et al. 2016; Klaus 2023). For each PHREEQC simulation, two  
323 files, respectively the database (with input reactions) and input files, were used to define the  
324 thermodynamic model and the type of calculations to perform. The database of MINTQA2 (e.g.,  
325 *minteq.dat*, Allison et al., 1991) was used to describe the chemical system because it includes, inter  
326 alia, reactions and constants for Ag, Cu and Hg complexation with Cl, NO<sub>3</sub> and carbonates.

327 Three PHREEQC simulations were run representing the addition of each preservative solution to  
328 sample water from Lake Svartkulp. The input files described the composition of two aqueous  
329 solutions: (i) the preservative solution assumed to contain only the preservative (i.e., HgCl<sub>2</sub> solution)  
330 and (ii) sample water from Lake Svartkulp with observed major element concentrations (pH, Al, Ca,  
331 Cl, Cu, Fe, Mg, Mn, N as nitrate, K, Na, S as sulfate, Zn; Tab. S1) and Hg and Ag natural  
332 concentration assumed to be 10<sup>-5</sup> mg/L. The output file provided the activities of the various solutes in  
333 the preserved samples, i.e., simulating the mixing of 120 mL of lake water with 240 µL of the AgNO<sub>3</sub>,  
334 CuCl<sub>2</sub> and HgCl<sub>2</sub> preservative solutions, as described in section 2.1. This procedure allows to estimate  
335 the pH of the preserved samples as well as SI for various mineral phases. The SI is calculated by  
336 PHREEQC comparing the chemical activities of the dissolved ions of a mineral (ion activity product,  
337 IAP) with their solubility product (K<sub>s</sub>). When SI > 1, precipitation is thermodynamically favourable.  
338 Note however that PHREEQC does not give information about precipitation kinetics.

339 Similarly, PHREEQC was used to estimate the decrease in pH caused by adding 150 µL of a half-  
340 saturated HgCl<sub>2</sub> solution to Lake Lundebyvannet samples prior to GC analyses, as described in  
341 section 2.2. In absence of data on the chemical composition of Lake Lundebyvannet, we assumed that  
342 it had the same composition as Lake Svartkulp water samples. This assumption is supported by the  
343 fact that waters from both lakes have circumneutral pH, low ionic strength (poor buffering capacity)  
344 and high DOC concentration and would therefore behave similarly in presence of acids. Briefly, for  
345 each 0.1 pH value between pH of 5.4 and 7.3, the carbonate alkalinity was first adjusted by increasing  
346 HCO<sub>3</sub> concentrations in the input files for PHREEQC to confirm that the water was at equilibrium at  
347 the given pH value. Then, the effect of adding 150µL of a half-saturated HgCl<sub>2</sub> solution was  
348 simulated as described above for Lake Svartkulp. Knowing the new equilibrated pH, after addition of

349 HgCl<sub>2</sub>, the overestimation of CO<sub>2</sub> concentration in Hg-fixed samples relative to unfixed samples (*E*,  
350 described in Eq. 8 above) can be predicted as described below.

351 Adapting Eq. (2), we obtain:

$$352 \quad [CO_2]_{HgCl_2} = \frac{[H^+]_{HgCl_2}^2 C_T}{Z_{HgCl_2}} \quad (\text{Eq. 9})$$

353 and

$$354 \quad [CO_2]_i = \frac{[H^+]_i^2 C_T}{Z_i} \quad (\text{Eq. 10})$$

355 where  $[H^+]_i$  is the proton concentration measured in the initial water samples prior to HgCl<sub>2</sub> fixation,  
356 and  $[H^+]_{HgCl_2}$  is the proton concentration estimated by PHREEQC following HgCl<sub>2</sub> fixation, and  
357 similarly for  $Z_i$  and  $Z_{HgCl_2}$  from Eq. (3). Combining Eqs. (7), (9) and (10) we obtain:

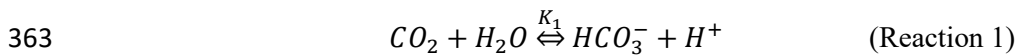
$$358 \quad [CO_2]_{ex} = C_T \left( \frac{[H^+]_{HgCl_2}^2}{Z_{HgCl_2}} - \frac{[H^+]_i^2}{Z_i} \right) \quad (\text{Eq. 11})$$

359 Hence:

$$360 \quad E = \frac{[CO_2]_{ex}}{[CO_2]_i} = \frac{\left( \frac{[H^+]_{HgCl_2}^2}{Z_{HgCl_2}} - \frac{[H^+]_i^2}{Z_i} \right)}{\frac{[H^+]_i^2}{Z_i}} \quad (\text{Eq. 12})$$

361

362 Alternatively, *E* can also simply be predicted based on the carbonic acid dissociation:



364 At equilibrium, we have:

$$365 \quad K_1 = \frac{[HCO_3^-][H^+]}{[CO_2]} \quad (\text{Eq. 13})$$

366 When pH is decreased upon addition of HgCl<sub>2</sub>, a fraction ( $\alpha$ ) of the initial bicarbonate concentration  
367  $[HCO_3^-]_i$  is turned into CO<sub>2</sub>. This fraction, expressed as  $[CO_2]_{ex}$  in Eq. (7) above, can be estimated  
368 with Eq. 13 as follows:

$$369 \quad [CO_2]_{ex} = \alpha [HCO_3^-]_i = \frac{\alpha K_1 [CO_2]_i}{[H^+]_i} \quad (\text{Eq. 14})$$

370 Introducing the expression of  $[CO_2]_{ex}$  from Eq. 14 into Eq. 8 yields:

$$371 \quad \frac{[CO_2]_{ex}}{[CO_2]_i} = E = \frac{\alpha K_1}{[H^+]_i} \quad (\text{Eq. 15})$$

372 When the decrease in pH, or acidification, is greater than the buffering capacity of the water:  $\alpha = 1$ .  
 373 The value of  $\alpha$  cannot exceed 1 because the amount of CO<sub>2</sub> produced by a decrease in pH cannot  
 374 exceed the amount of  $HCO_3^-$  initially present. In all the other cases, we have:  $\alpha < 1$ . For both  
 375 predictions of  $E$ , i.e., with Eqs. 12 and 15, the root-mean-square error (RMSE) and coefficient of  
 376 determination ( $R^2$ ) were calculated.

377 Finally, additional sources of CO<sub>2</sub> overestimation were investigated by analysing the residuals of the  
 378 model described by Eq. 12, i.e., the difference between  $E$  predicted with Eq. 12 and  $E$  determined  
 379 empirically with Eq. 8. Briefly, residuals were plotted against pH and *in situ* temperature. Residuals  
 380 were separated in two groups based on the empirical value of  $[HCO_3^-]_i - [CO_2]_{ex}$ , i.e., the first group  
 381 had values of  $[HCO_3^-]_i - [CO_2]_{ex} \geq a$  while the second group had values of  $[HCO_3^-]_i - [CO_2]_{ex} \leq$   
 382  $-a$  where different values for  $a$  were used: 20, 10 or 5  $\mu\text{M}$ . The justification for separating residuals  
 383 in two groups is that: (i) the first group represents samples for which bicarbonate alkalinity in the  
 384 original sample is, as expected, higher than CO<sub>2</sub> overestimation after HgCl<sub>2</sub>-fixation, while (ii) the  
 385 second group represents samples for which bicarbonate alkalinity is not sufficient to explain CO<sub>2</sub>  
 386 overestimation after HgCl<sub>2</sub>-fixation.

387

### 388 *CO<sub>2</sub> diffusion fluxes from Lake Lundebyvannet*

389 The diffusive flux of CO<sub>2</sub> ( $F_{CO_2}$  in mol m<sup>-2</sup> d<sup>-1</sup>) from Lake Lundebyvannet surface water was  
 390 estimated according to:

$$391 \quad F_{CO_2} = \frac{k_{CO_2}([CO_2] - [CO_2]_{eq})}{1000} \quad (\text{Eq. 16})$$

392 where  $k_{CO_2}$  is the CO<sub>2</sub> transfer velocity in m d<sup>-1</sup>,  $[CO_2]$  is the surface water CO<sub>2</sub> concentration ( $\mu\text{M}$ ),  
 393 and 1000 is a factor to ensure consistency in the units and  $[CO_2]_{eq}$  is the theoretical water CO<sub>2</sub>  
 394 concentration ( $\mu\text{M}$ ) in equilibrium with atmospheric CO<sub>2</sub> concentration calculated with Eq. (3) and  
 395 pCO<sub>2</sub> of 416  $\mu\text{atm}$  (see above).

396 The CO<sub>2</sub> transfer velocity ( $k_{CO_2}$ ) was estimated as follows (Vachon & Prairie, 2013):

$$397 \quad k_{CO_2} = k_{600} \left( \frac{600}{Sc_{CO_2}} \right)^{-n} \quad (\text{Eq. 17})$$

398 where  $k_{600}$  is the gas transfer velocity (m d<sup>-1</sup>) estimated from empirical wind-based models and  $Sc_{CO_2}$   
 399 is the CO<sub>2</sub> Schmidt number for *in situ* water temperature (unitless; Wanninkhof, 2014). We used  $n$   
 400 values of 0.5 or 2/3 when wind speed was below or above 3.7 m s<sup>-1</sup>, respectively (Guérin et al., 2007).  
 401 Empirical  $k_{600}$  models included those from Cole & Caraco (1998;  $k_{600} = 2.07 + 0.215U_{10}^{1.7}$ ),  
 402 Vachon & Prairie (2013;  $k_{600} = 2.51 + 1.48U_{10} + 0.39U_{10} \log_{10} LA$ ) and Crusius & Wanninkhof

403 (2003; power model:  $k_{600} = 0.228U_{10}^{2.2} + 0.168$  in cm h<sup>-1</sup>).  $U_{10}$  and  $LA$  refer to mean wind speed at  
404 10 m in m s<sup>-1</sup> and lake area in km<sup>2</sup>, respectively. Sub-hourly  $U_{10}$  data for 2020 was retrieved from a  
405 weather station of the Norwegian Meteorological Institute located 1.5 km west of Lake  
406 Lundebyvannet (station name: E18 Melleby; ID: SN 3480; 59.546 N, 11.4535E) using the Frost  
407 application programming interface (*Frost API*, 2022). Daily, monthly, and yearly (only covering the  
408 ice-free season: April-November)  $F_{CO_2}$  was estimated using Eq. (12). Daily [CO<sub>2</sub>] was interpolated  
409 from weekly data using a modified Akima spline (makima spline in Matlab® based on Akima, 1974).  
410 This interpolation method is known to avoid excessive local undulations.

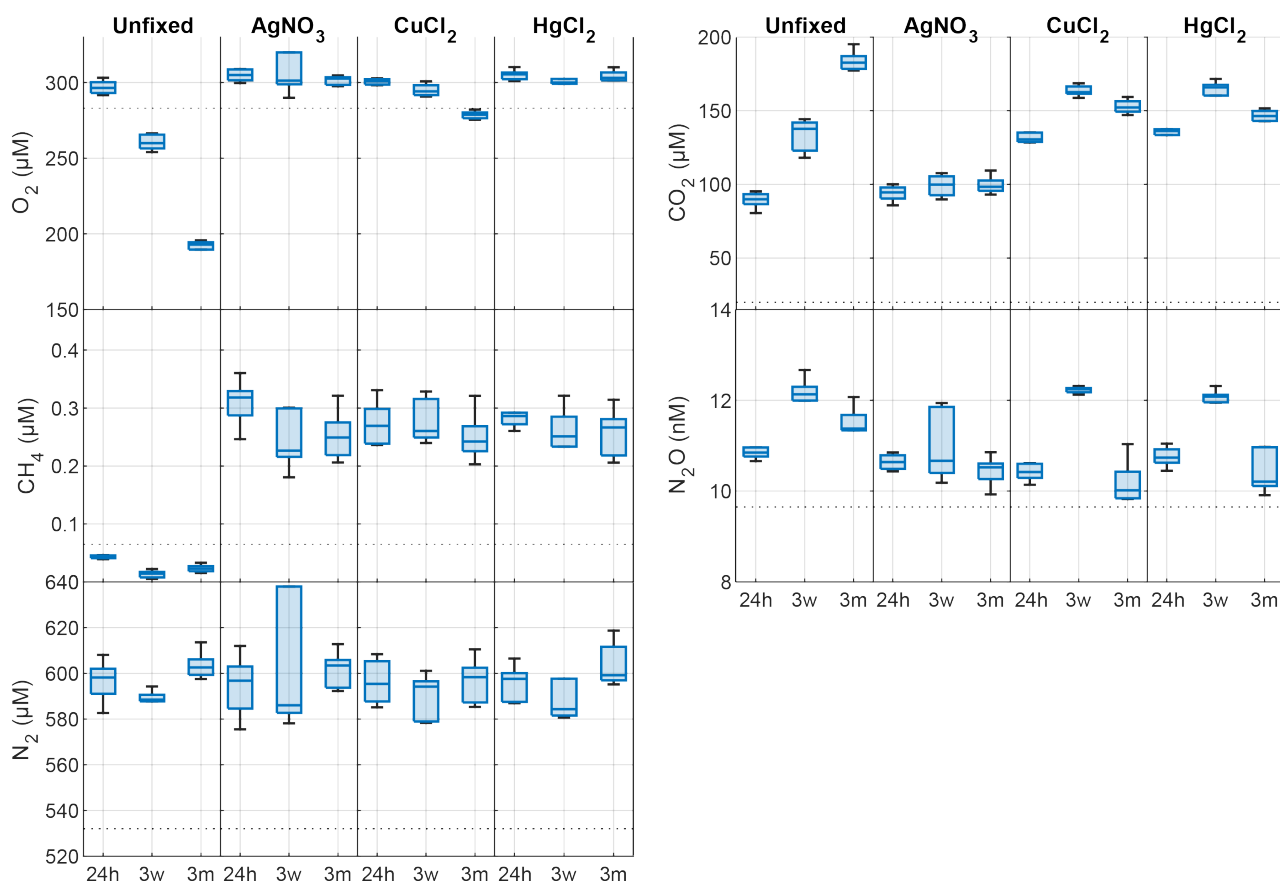
### 411 3. Results

#### 412 3.1. Effects of preservatives and storage time on dissolved gases

413 In the unfixed samples from Lake Svartkulp, the concentration of O<sub>2</sub> declined while CO<sub>2</sub> increased  
414 over time in a close to 1:1 molar ratio, likely reflecting the effect of microbial respiration activity and  
415 mineralisation of organic matter (Fig. 2, Tab. S2). Concentration of O<sub>2</sub> in the unfixed samples  
416 decreased from near 300 to below 200 μM (Fig. 2). In the presence of inhibitors, O<sub>2</sub> concentrations  
417 tended to be slightly higher at t=24h and remained constant or declined only slightly over time to  
418 generally remain at or above saturation (280 to 300 μM). Thus, the inhibitors were effective in  
419 reducing oxic respiration.

420 The concentration of CO<sub>2</sub> in the presence of AgNO<sub>3</sub> at t = 24h was not significantly different to the  
421 unfixed at t = 0 (Fig 2; paired t-test,  $P > 0.1$ ). At t = 24h, CO<sub>2</sub> concentrations were however much  
422 higher in the presence of HgCl<sub>2</sub> (135 μM) or CuCl<sub>2</sub> (131 μM) than in the unfixed (89 μM; Fig 2, Tab.  
423 S2). The CO<sub>2</sub> further increases from 130 μM to ~160 μM after 3 weeks in both sample sets preserved  
424 with HgCl<sub>2</sub> and CuCl<sub>2</sub> while a decrease in O<sub>2</sub> is less pronounced for samples fixed with CuCl<sub>2</sub> and  
425 completely absent for samples fixed with HgCl<sub>2</sub>. Overall, the addition of HgCl<sub>2</sub> or CuCl<sub>2</sub> following  
426 sampling increased CO<sub>2</sub> concentrations by 47% after 24h compared to the unfixed and caused further  
427 changes over the three-month storage time, while preservation with AgNO<sub>3</sub> yielded CO<sub>2</sub>  
428 concentrations consistent with the unfixed and caused negligible changes over time (Fig. 2; paired t-  
429 test,  $P > 0.1$ ).

430 The concentration of CH<sub>4</sub> across all samples ranged between 0.017 and 0.377 μM (Fig. 2), as  
431 expected two orders of magnitude smaller than CO<sub>2</sub>. At t = 24h, the concentration of CH<sub>4</sub> was over  
432 0.2 μM in the presence of inhibitors while it was below saturation in the unfixed (0.03 μM; Fig. 2).  
433 CH<sub>4</sub> oversaturation in the preserved samples persisted after three weeks and three months of storage  
434 and CH<sub>4</sub> concentration remained unchanged (Fig. 2, Tab. S2).



435

436 **Fig 2.** Changes in dissolved O<sub>2</sub>, CO<sub>2</sub>, CH<sub>4</sub>, N<sub>2</sub>O and N<sub>2</sub> concentrations (nM or µM) in the absence  
 437 (unfixed) and presence of different preservatives (AgNO<sub>3</sub>, CuCl<sub>2</sub>, HgCl<sub>2</sub>) at three times (24h, 24h  
 438 after incubation start; 3w, three weeks after collection; 3m, three months after collection). The  
 439 horizontal dotted line is the saturated gas concentration corresponding to 100% gas saturation at *in*  
 440 *situ* lake temperature. Box plots show the median, 25<sup>th</sup> and 75<sup>th</sup> percentiles and the whiskers display  
 441 minimum and maximum.



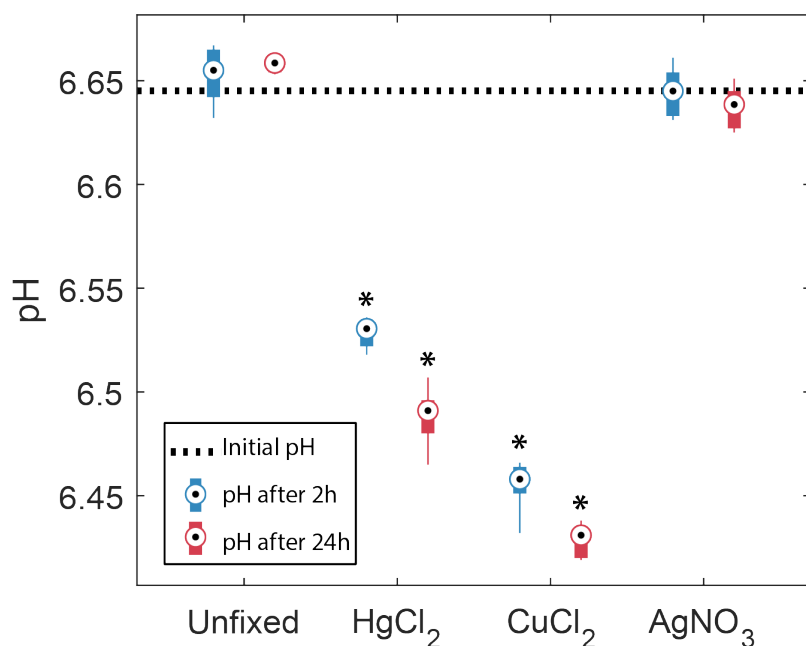
442 The concentration of N<sub>2</sub>O ranged between 9.8 and 12.7 nM with only samples preserved with AgNO<sub>3</sub>  
 443 showing negligible changes over time (Fig. 2; paired t-test, P>0.1). All the other samples showed  
 444 consistent patterns with storage time. N<sub>2</sub>O concentrations initially increased within the first 3 weeks,  
 445 followed by a decrease after 3 months.

446 The changes in N<sub>2</sub> were likely within handling and analytical errors and not different in the presence  
 447 or absence of inhibitors (Fig. 2; Tab. S2; paired t-test, P>0.1).

448

### 449 3.2. Effects of preservatives on pH

450 In the samples amended with ultrapure water or AgNO<sub>3</sub>, the pH did not show any significant changes  
 451 after 2h or 24h. In contrast, both groups with HgCl<sub>2</sub> and CuCl<sub>2</sub> treatments show significant decreases  
 452 of pH after 2h, -0.12 and -0.19, respectively, and 24h, -0.16 and -0.21, respectively. In addition, they  
 453 showed a significant decrease in pH from 2h to 24h. Samples amended with CuCl<sub>2</sub> show the strongest  
 454 decrease in pH.



455

456 **Fig 3.** Observed changes in pH in the absence (unfixed) and presence of different preservatives  
 457 (AgNO<sub>3</sub>, CuCl<sub>2</sub>, HgCl<sub>2</sub>) at two times, 2h and 24h after the start of the incubation. The horizontal  
 458 dotted line represents the initial pH of the bulk water sample. Box plots show the median, 25<sup>th</sup> and  
 459 75<sup>th</sup> percentiles and the whiskers display minimum and maximum of the 6 replicates. Stars indicate  
 460 groups that are significantly different from each other and from the initial pH (two-way ANOVA).

461 3.3. Contrasting impacts of HgCl<sub>2</sub>, CuCl<sub>2</sub> and AgNO<sub>3</sub> on dissolved CO<sub>2</sub> estimation revealed by  
 462 chemical speciation modelling

463 The PHREEQC simulation of unpreserved samples, based on concentrations of all major elements  
 464 (Tab. S1), predicted a pH of 6.72 (Tab. 2) which is very close to the measured pH of 6.73 (Tab. S1).  
 465 This suggests that chemical information provided to PHREEQC is likely sufficient to describe the  
 466 system, without having to invoke more complex reactions with dissolved organic matter. The addition  
 467 of HgCl<sub>2</sub> and CuCl<sub>2</sub> both caused a significant decrease in pH to 6.40 and 6.45, respectively (Tab. 2)  
 468 which is similar to the decrease observed at the end of the 24h short term incubation (Fig. 2).

469 In absence of preservatives, none of the common carbonate minerals, including calcite, were  
 470 associated with a saturation index higher than 1, i.e., dissolution was thermodynamically favourable  
 471 for all these minerals and no DIC loss was expected (Tab. 2). However, upon addition of HgCl<sub>2</sub> or  
 472 CuCl<sub>2</sub>, some carbonate minerals, e.g., HgCO<sub>3</sub> or malachite and azurite, respectively, were expected to  
 473 spontaneously precipitate given their relatively high saturation index values.

474 **Tab. 2.** pH and saturation indices of selected carbonate minerals estimated by PHREEQC for the  
 475 unpreserved and preserved samples

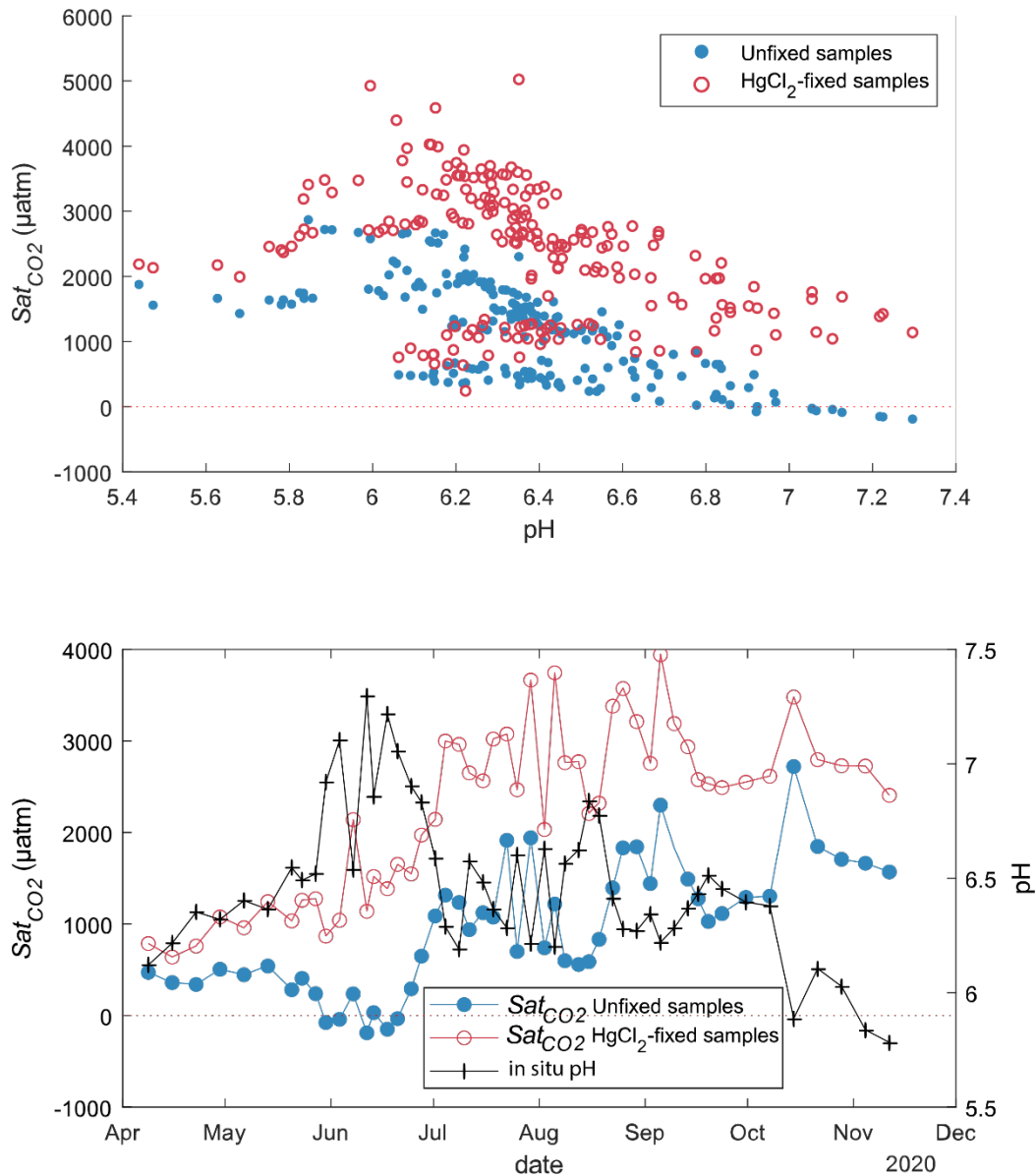
Preservatives	pH	Saturation indices			
		HgCO <sub>3</sub>	Cu <sub>2</sub> (OH) <sub>2</sub> CO <sub>3</sub> - Malachite	Cu <sub>2</sub> (OH) <sub>2</sub> CO <sub>3</sub> - Azurite	Ag <sub>2</sub> CO <sub>3</sub>
Unfixed	6.72	-2.31	-4.96	-8.71	-16.42
HgCl <sub>2</sub>	6.40	3.64	-5.89	-10.10	-17.20
CuCl <sub>2</sub>	6.45	-2.55	2.26	2.11	-17.44
AgNO <sub>3</sub>	6.71	-2.31	-4.97	-8.73	-4.33

476

### 477 3.3. Effects of HgCl<sub>2</sub> on dissolved CO<sub>2</sub> concentration under a range of pH

478 CO<sub>2</sub> concentrations in unfixed water samples from Lake Lundebyvannet were significantly lower than  
 479 in the HgCl<sub>2</sub>-fixed samples (mean difference: 52 μM; paired t-test; P<0.0001; Tab. 3). Fixation with  
 480 HgCl<sub>2</sub> caused a general overestimation of CO<sub>2</sub> concentration and the saturation deficit (Fig. 4), thus  
 481 missing out events of CO<sub>2</sub> influx (carbon sink) under high photosynthesis activity (high pH; Fig. 4).  
 482 In parallel, PHREEQC predicted a decrease of 0.6 to 1.8 units of pH related to HgCl<sub>2</sub> addition (Fig.  
 483 S1).

484



485

486 **Fig. 4.** CO<sub>2</sub> saturation deficit ( $Sat_{CO_2}$ ) in Lake Lundebyvannet as a function of in situ pH for all  
 487 unfixed (obtained from DIC analysis) and HgCl<sub>2</sub>-fixed (obtained from GC analysis) samples (top  
 488 panel). Timeseries of pH and CO<sub>2</sub> saturation deficit of surface water (1-m deep) for unfixed and  
 489 HgCl<sub>2</sub>-fixed samples (bottom panel).

490 **Tab. 3.** CO<sub>2</sub> concentrations ([CO<sub>2</sub>], μM) and diffusion fluxes (F<sub>CO<sub>2</sub></sub>, mol m<sup>-2</sup> d<sup>-1</sup>) from Lake Lake  
 491 Lundebyvannet estimated from HgCl<sub>2</sub>-fixed and unfixed samples following Cole and Caraco (1998).  
 492 Ice-free season spans April to November. Data are also shown in Fig. 6.

Preservatives		Apr.	May	Jun.	Jul.	Aug.	Sep.	Oct.	Nov.	Ice-free season
[CO <sub>2</sub> ]	None	45	39	19	68	59	85	123	120	67
	HgCl <sub>2</sub>	68	75	74	133	130	149	179	178	121
	Diff (%)	+50	+93	+296	+96	+119	+75	+45	+49	+82
F <sub>CO<sub>2</sub></sub>	None	0.10	0.07	0.01	0.15	0.11	0.23	0.37	0.48	0.17
	HgCl <sub>2</sub>	0.20	0.21	0.16	0.34	0.29	0.47	0.57	0.77	0.35
	Diff (%)	+97	+188	+2163	+130	+162	+99	+55	+62	+108

493 The pH value of water samples from Lake Lundebyvannet varied between 5.4 and 7.3 (Fig 4 and 5),  
 494 mainly due to marked variations in phytoplankton photosynthetic activity (Rohrlack et al., 2020). The  
 495 relative overestimation of CO<sub>2</sub> (*E*) follows an exponential increase with pH and is well reproduced by  
 496 a simple exponential function ( $2.56 \times 10^{-5} \times 10^{1.015 \times pH}$ , RMSE=44%, R<sup>2</sup>=0.81, p<0.0001; Fig. 5).

497

#### 498 4. Discussion

499 Prior to using dissolved gas concentrations in freshwater to estimate the magnitude of biological  
 500 aquatic processes such as photosynthesis and oxic respiration, denitrification and methanogenesis, we  
 501 must ensure that biological activity between sampling and laboratory analyses was efficiently  
 502 inhibited without significant impacts on the sample's chemistry. Here we report a unique dataset on  
 503 the impact of three preservatives on water samples from a typical low-ionic strength, unproductive  
 504 boreal lake to inform on potential risks of mis-estimation of dissolved gas concentrations. We further  
 505 show, using CO<sub>2</sub> concentration data from a typical productive boreal lake, that using HgCl<sub>2</sub> can lead  
 506 to negligence of the role of photosynthesis in lake C cycling.

##### 507 4.1 Best preservative for the determination of dissolved gas concentrations

508 Given that none of the four treatments (unfixed, HgCl<sub>2</sub>, CuCl<sub>2</sub> or AgNO<sub>3</sub>) applied to Lake Svartkulp  
 509 water samples during the 3-month incubation offer an independent control, a first challenge is to  
 510 determine which of the treatment represent the most realistic dissolved gas concentrations close to  
 511 real condition. For CO<sub>2</sub> and O<sub>2</sub>, a few studies have used unfixed samples (only preserved dark at  
 512 +4°C) up to 48h after sampling to determine CO<sub>2</sub> or DIC concentrations (e.g., Sobek et al. 2003,  
 513 Kocik et al., 2015). So, the CO<sub>2</sub> and O<sub>2</sub> concentrations in the unfixed samples collected after 24h  
 514 incubation are the most representative of the initial real concentrations. Biological activity might have  
 515 had an impact, but this is likely negligible over the first 24h. In addition, the fact that the CO<sub>2</sub> and O<sub>2</sub>

516 concentrations in the samples fixed with AgNO<sub>3</sub> after 24h, three weeks and three months are equal to  
517 those from unfixed samples after 24h (Fig. 2) confirms that the unfixed samples after 24h can be used  
518 as a control. In fact, only samples fixed with AgNO<sub>3</sub> are trustful given the expected toxicity of Ag, the  
519 absence of impact on pH (Fig. 3), and unchanged concentrations over the three-month experiment for  
520 all gases. Similarly, N<sub>2</sub>O and N<sub>2</sub> concentrations in the unfixed samples after 24h can be used as  
521 control. However, for CH<sub>4</sub>, Fig. 2 shows that already after 24h, the CH<sub>4</sub> concentration in the unfixed  
522 samples is below atmospheric saturation while it is consistently much higher in all three sets of fixed  
523 samples. Boreal lakes are typically over saturated with respect to CH<sub>4</sub> (Valiente et al., 2022) and it is  
524 very unlikely that CH<sub>4</sub> could have been produced in lake water incubated under high concentration of  
525 oxygen and toxic preservatives. Hence, unfixed samples do not represent real CH<sub>4</sub> concentrations.  
526 These observations are all consistent with the fact that the three preservatives were effective in  
527 preserving CH<sub>4</sub> from oxidation. Even over 24h, preservatives need to be added to oxic water samples  
528 to preserve CH<sub>4</sub> from oxidation. In fact, oxic methanotrophy typically show rates in the order of μM  
529 day<sup>-1</sup> (Thottathil et al., 2019; van Grinsven et al., 2021). Hence, a CH<sub>4</sub> consumption of 0.3 μM within  
530 24h in the unfixed water samples is realistic (Fig. 2).

531 In summary, preservation with AgNO<sub>3</sub> is the only method that offered robust determination of all five  
532 dissolved gases with negligible changes in concentration over time.

#### 533 4.2 Risks of mis-estimating dissolved gas concentration with HgCl<sub>2</sub> and CuCl<sub>2</sub> preservation

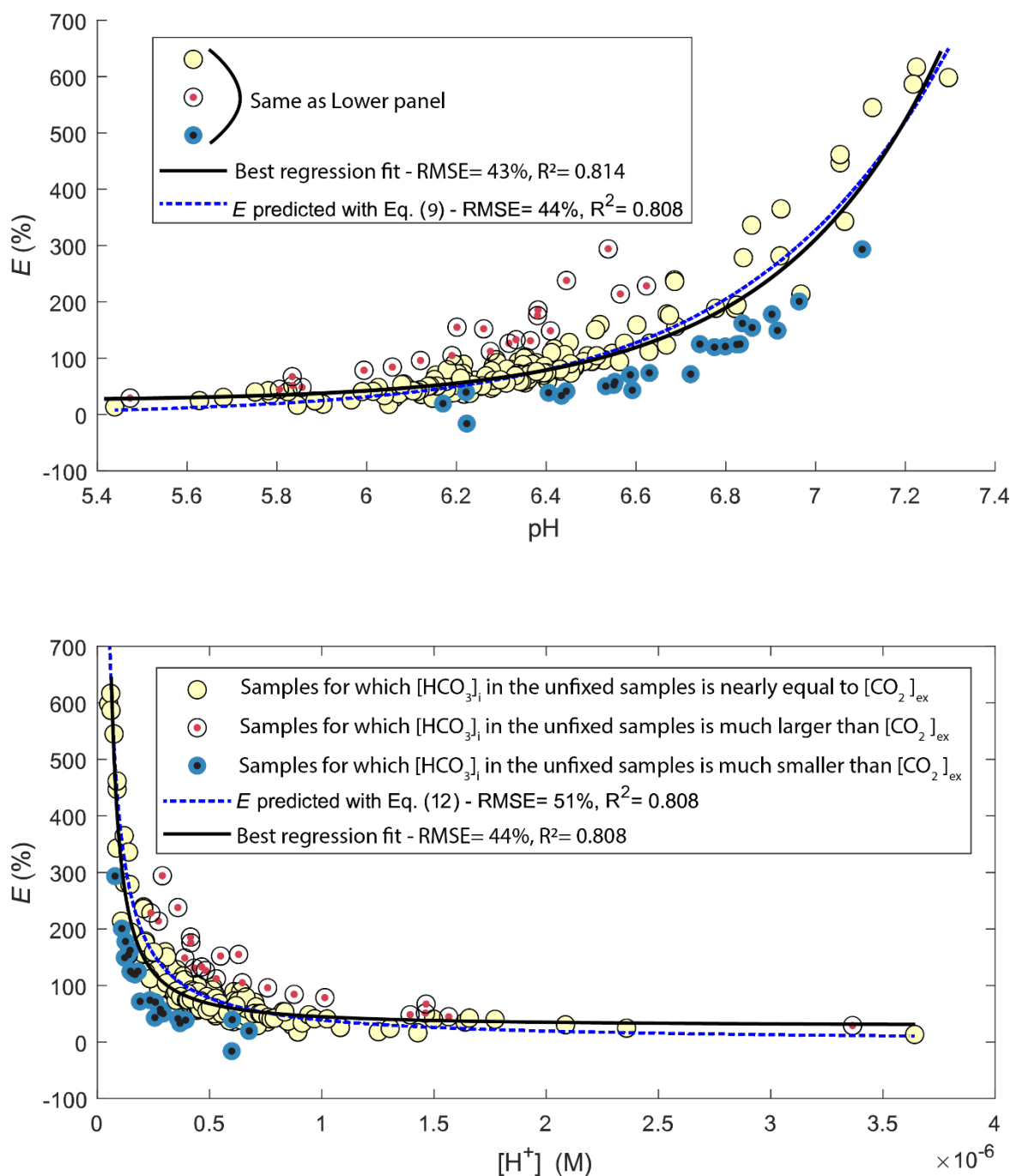
534 Both sets of samples preserved with either HgCl<sub>2</sub> and CuCl<sub>2</sub> showed CO<sub>2</sub> concentrations that were  
535 much higher than the unfixed (after 24h) or the AgNO<sub>3</sub>-fixed samples. This is due to an acidification  
536 of the poorly buffered (alkalinity 127 μM) and near neutral water (pH=6.73), shifting the carbonate  
537 equilibrium from HCO<sub>3</sub><sup>-</sup> to CO<sub>2</sub> as also shown by Borges et al. (2019). In fact, a rapid decrease in pH  
538 was observed upon HgCl<sub>2</sub> and CuCl<sub>2</sub> treatments (Fig. 3). The increase of CO<sub>2</sub> from about 130 μM to  
539 ~160 μM after 3 weeks in both sample sets preserved with HgCl<sub>2</sub> and CuCl<sub>2</sub> is not mirrored by a  
540 similar decrease in O<sub>2</sub> (Fig. 2). This suggests that oxic respiration is not the main source for this  
541 additional 30 μM of CO<sub>2</sub> but rather points towards additional acidification of the samples caused, e.g.,  
542 by kinetically controlled complexation of Hg<sup>2+</sup> with dissolved organic matter (Miller et al., 2009). In  
543 fact, the relatively slow complexation of Hg<sup>2+</sup> with organic thiol groups can release two protons  
544 (Skylberg, 2008) and up to three, with some participation of a third weak-acid group (Khwaja et al.,  
545 2006). The transient nature of acidification caused by HgCl<sub>2</sub> and CuCl<sub>2</sub> is also evident in the pH  
546 impacts showing higher acidification after 24h than after 2h incubation (Fig. 3). The following  
547 decrease in CO<sub>2</sub> after 3 months (down to ~145 μM) points to other processes. The precipitation of Hg  
548 and Cu carbonates, given their high saturation index values (Tab. 2), would be consistent with the  
549 decrease in CO<sub>2</sub> concentrations observed between three weeks and three months. Calcite precipitation  
550 is typically observed in supersaturated solutions within 48h (Kim et al., 2020). Hence, it is realistic to

551 consider that Hg and Cu carbonate precipitation influenced the CO<sub>2</sub> concentration within the  
552 preserved samples over the three months of storage time. Impacts of Hg or Cu carbonate precipitation  
553 is not evident after three weeks likely because of slow but persistent CO<sub>2</sub> production in presence of  
554 HgCl<sub>2</sub> and CuCl<sub>2</sub> related to acidification as described above (Fig. 2). However, after three weeks, this  
555 production likely weakens and is counterbalanced by increasing carbonate precipitation.

556 Overall, the addition of HgCl<sub>2</sub> or CuCl<sub>2</sub> following sampling increased CO<sub>2</sub> concentrations by 47%  
557 within the first 24h compared to the unfixed consistent with the -0.16 to -0.21 pH-unit acidification  
558 observed over the same time in the pH incubation experiment (Fig. 3) and the pH estimated with  
559 PHREEQC without the interaction with dissolved organic matter (Tab. 2). In fact, introducing pH and  
560 CO<sub>2</sub> concentration values of 6.40–6.45 and 130 μM, respectively, for the samples preserved with  
561 HgCl<sub>2</sub> and CuCl<sub>2</sub> into Eqs. 1 and 2 yields DIC concentrations (C<sub>T</sub>) of about 270 μM at t=24h. These  
562 DIC concentrations are almost equal to those calculated for the unfixed samples and those preserved  
563 with AgNO<sub>3</sub> at t = 24h, i.e., with a pH of 6.73 and CO<sub>2</sub> concentration of 88 μM. Interestingly, the  
564 concentration of CO<sub>2</sub> in the samples preserved with HgCl<sub>2</sub> and CuCl<sub>2</sub> continues to increase up to ~160  
565 μM after 3 weeks. Given that oxic respiration is inhibited (Fig. 2), this additional CO<sub>2</sub> is believed to  
566 originate from progressive release of protons following relatively slow complexation of Hg<sup>2+</sup> with  
567 dissolved organic matter (Khwaja et al., 2006; Miller et al., 2009; Skjellberg, 2008). Note however  
568 that this process could not be predicted with PHREEQC given that it neglected the effect of dissolved  
569 organic matter.

570 Unlike the AgNO<sub>3</sub>-fixed samples, all the other samples showed an initial increase in N<sub>2</sub>O  
571 concentration from 24h to 3 weeks, followed by a decrease from three weeks to 3 months. Similar  
572 patterns of net N<sub>2</sub>O production followed by net consumption were also reported in short-term  
573 incubations of seawater from the high latitude Atlantic Ocean, although over much shorter timescales,  
574 i.e., 48 and 96h (Rees et al., 2021). The large difference in kinetics between the latter experiment  
575 (Rees et al., 2021) and our incubation might be attributable to differences in incubation temperature  
576 where the seawater from the high latitude Atlantic Ocean was incubated at ambient temperatures  
577 while our samples were kept at +4°C. Other difference in the experimental setup might have also  
578 played a role. The lack of inhibition of N<sub>2</sub>O production and consumption in the samples preserved  
579 with HgCl<sub>2</sub> and CuCl<sub>2</sub> can be attributed to the fact that N<sub>2</sub>O production tends to increase under  
580 increasing acidic conditions (Knowles, 1982; Mørkved et al., 2007; Seitzinger, 1988). In fact, the  
581 mole fraction of N<sub>2</sub>O produced during denitrification increases compared to N<sub>2</sub> as pH decreases  
582 (Knowles, 1982).

583



584

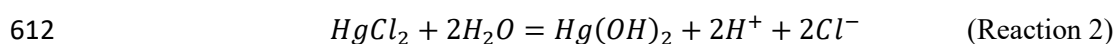
585 **Fig. 5.** Comparison of observed (circles) and predicted (blue line) relative overestimation ( $E$ ) of CO<sub>2</sub>  
 586 concentrations caused by HgCl<sub>2</sub> fixation in Lake Lundebyvannet samples as a function of pH (top  
 587 panel) or proton concentration (bottom panel). The black line shows the best fit of the regression  
 588 analysis. White symbols represent samples for which the bicarbonate concentration in the unfixed  
 589 samples ( $[HCO_3^-]_i$ ) is nearly equal to CO<sub>2</sub> overestimation ( $[CO_2]_{ex}$ ), i.e.,  $\pm 20\mu\text{M}$  (equivalent to a pH  
 590 error of 0.05), while red and blue symbols represent samples for which initial bicarbonate  
 591 concentration was lower and higher than the CO<sub>2</sub> overestimation, respectively.

592 4.3 Using PHREEQC to estimate acidification caused by HgCl<sub>2</sub> in samples from Lake Lundebyvannet

593 As for the samples from Lake Svartkulp as described above, the overestimation of CO<sub>2</sub> concentration  
 594 in the samples from Lake Lundebyvannet fixed with HgCl<sub>2</sub> (161 μM added; Fig. 4) likely stems from  
 595 the acidification shifting the carbonate equilibrium from bicarbonate to CO<sub>2</sub>. In fact, PHREEQC  
 596 predicted a decrease of 0.6 to 1.8 units of pH related to HgCl<sub>2</sub> addition in these samples (Fig. S1).

597 The relative overestimation of CO<sub>2</sub> (*E* in Fig. 5) followed a typical exponential increase reflecting the  
 598 decrease in absolute CO<sub>2</sub> concentration with increasing pH (Stumm & Morgan, 1981) caused here by  
 599 phytoplankton photosynthesis. In fact, the exponential increase in CO<sub>2</sub> overestimation is easily  
 600 predicted by Eq. (9) with an equivalent level of accuracy as the optimized exponential function (Fig.  
 601 5). Consistently, the relative overestimation of CO<sub>2</sub> (*E*) shows an inverse decrease with [H<sup>+</sup>] that is  
 602 well reproduced by a simple inverse function ( $3.25 \times 10^{-5}/[H^+]$ ; RMSE=44%, R<sup>2</sup>=0.81, p<0.0001;  
 603 Fig. 5) and predicted by Eq. (15), with an α value of 1. Combining Eqs. 8 and 15 and solving it with  
 604 pH values estimated from PHREEQC (Fig. S1) for α yields values ranging between 0.72 and 0.89  
 605 with an average of 0.85. Unexpectedly, this average α value is almost equal to the ratio of the inverse  
 606 function coefficient and K<sub>1</sub>, i.e.,  $\frac{3.25 \times 10^{-5}}{K_1} = 0.87$ . Hence, the relative overestimation of CO<sub>2</sub> (*E*)  
 607 caused by HgCl<sub>2</sub> fixation is easily predicted by the change in bicarbonate equilibrium knowing the  
 608 proton release from HgCl<sub>2</sub> addition, here estimated with PHREEQC.

609 Hence, PHREEQC can be used to predict decrease in pH caused by HgCl<sub>2</sub> fixation, if sufficient  
 610 knowledge is gathered on the ionic water composition. Proton release during HgCl<sub>2</sub> fixation can be  
 611 represented by the following reaction:



613 From reaction 2, it becomes evident that the initial concentration of chloride in the water samples will  
 614 likely limit HgCl<sub>2</sub> dissociation and proton release. This is a likely mechanism occurring in seawater  
 615 where HgCl<sub>2</sub> has been shown to cause a decrease in pH, although at a negligible level with a  
 616 maximum decrease in pH of -0.01 (Chou et al., 2016).

617 Figure 3 shows that a range of water samples were associated with a relative CO<sub>2</sub> overestimation (*E*)  
 618 that substantially deviated from the overestimation predicted with Eq. 12 (red and blue symbols in  
 619 Fig. 5). In fact, some samples had a higher initial bicarbonate content ( $[HCO_3^-]_i$ ) than the excess CO<sub>2</sub>  
 620 concentration ( $[CO_2]_{ex}$ ), while other showed the opposite. The former case (blue symbols in Fig. 5)  
 621 can easily be explained by a higher buffering capacity of the sampled water, i.e., a higher pH after  
 622 HgCl<sub>2</sub>-fixation than that predicted by PHREEQC related to a different water composition. Indeed, the  
 623 concentration of major elements in the water from Lake Lundebyvannet may vary significantly over  
 624 time, and in absence of data, we considered that the water composition, except for DIC, pH and



625 HgCl<sub>2</sub>, was constant over time. By contrast, samples associated with  $[CO_2]_{ex}$  being larger than  
626  $[HCO_3^-]_i$  are more enigmatic. In order to shed light on possible explanations, we visually inspected  
627 trends between empirical deviations from predictions, i.e., residuals, and *in situ* temperature or pH.  
628 Absolute values of residuals showed a progressive increase with pH and *in situ* temperature which is  
629 in agreement with decreasing precision of the headspace method with increasing temperature and pH  
630 (Koschorreck et al., 2021). In fact, CO<sub>2</sub> is less soluble at higher temperature, hence more gas can  
631 evade during sampling, and thus the error increases with *in situ* temperature. In addition, at higher pH,  
632 CO<sub>2</sub> concentration decreases and consequently the absolute error on CO<sub>2</sub> quantification becomes  
633 larger relative to measured CO<sub>2</sub> concentration. Interestingly, many of the high residual values were  
634 not evenly distributed across the year, nor across the summer and were rather associated with only a  
635 few specific sampling events during summer (Fig. S2). This suggests that degassing could have  
636 occurred due to high ambient temperature in the field. Water associated with  $[CO_2]_{ex}$  being larger  
637 than  $[HCO_3^-]_i$  (red symbols in Fig. 5 and S4) could have been subject to a larger degassing in the  
638 samples collected for DIC analysis than the samples for GC analysis. On the other hand, degassing  
639 was likely larger for samples for GC analysis than for DIC analysis for water associated with  
640  $[HCO_3^-]_i$  being larger than  $[CO_2]_{ex}$  (blue symbols in Fig. 5 and Fig. S2). In addition to degassing and  
641 temperature effects, errors in pH measurements can also cause a large misestimation of CO<sub>2</sub>  
642 concentration from DIC analysis, and this error increases exponentially with pH following the shift in  
643 carbonate equilibrium. In summary, our analysis is consistent with that of Koschorreck et al. (2021)  
644 showing that errors in the determination of CO<sub>2</sub> concentrations are smaller at lower pH and lower  
645 temperature (Fig. S2).

#### 646 4.4. Implications for the estimation of lake and reservoir C cycling and recommendations

647 Using HgCl<sub>2</sub> or CuCl<sub>2</sub> to preserve dissolved gas samples in poorly buffered water samples has large  
648 impacts on CO<sub>2</sub> concentrations with considerable risk of leading to incorrect interpretations. The risk  
649 of mis-estimating CO<sub>2</sub> concentration due to HgCl<sub>2</sub> and CuCl<sub>2</sub> preservation is the highest when pH of  
650 the unfixed water is close to the first carbonic acid dissociation constant ( $pK_1 = 6.41$  at 25°C; Stumm  
651 & Morgan, 1996). It implies that any small shift in pH will have a significant impact in the carbonate  
652 equilibrium between bicarbonate to CO<sub>2</sub>. The risk is also the highest in the lowest ionic strength  
653 waters. In that respect, low-ionic strength, slightly acidic to neutral, moderately humic lakes  
654 commonly found in Norway (de Wit et al., 2023), large parts of Sweden (Valina et al. 2014), and  
655 Finland, Atlantic Canada (Houle et al., 2022), Ontario, Québec, and North-East USA (Skjelkvåle and  
656 de Wit 2011; Weyhenmeyer et al., 2019) are the most prone to errors in CO<sub>2</sub> concentrations related to  
657 HgCl<sub>2</sub> or CuCl<sub>2</sub> preservation. Through a preliminary literature search we found several studies from  
658 boreal lakes (Jonsson et al., 2001; Urabe et al., 2011; Yang et al., 2015; Hessen et al., 2017) but also  
659 from circum-neutral pH sub-tropical to tropical aquatic environments (Jeffrey et al., 2018; Webb et  
660 al., 2018; Ray et al., 2021) where preservation with HgCl<sub>2</sub> may have caused biases in the

661 quantification of CO<sub>2</sub> concentrations as it was the case for samples from the Congo River (Borges et  
662 al., 2019). A significant part of the low-ionic strength boreal lakes become increasingly sensitive to  
663 changes in nutrients with strong impacts on their role in carbon cycling (Myrstener et al., 2022). In  
664 this context, it is crucial to avoid mis-estimation of CO<sub>2</sub> concentrations and thus avoid use of HgCl<sub>2</sub> or  
665 CuCl<sub>2</sub> to ensure a robust understanding of the role of autotrophic processes in lake C cycling. Below  
666 we describe the implications for the lake C budget of Lundebyvannet as an example of a mis-  
667 estimation of the role of photosynthesis in a typical productive boreal lake.

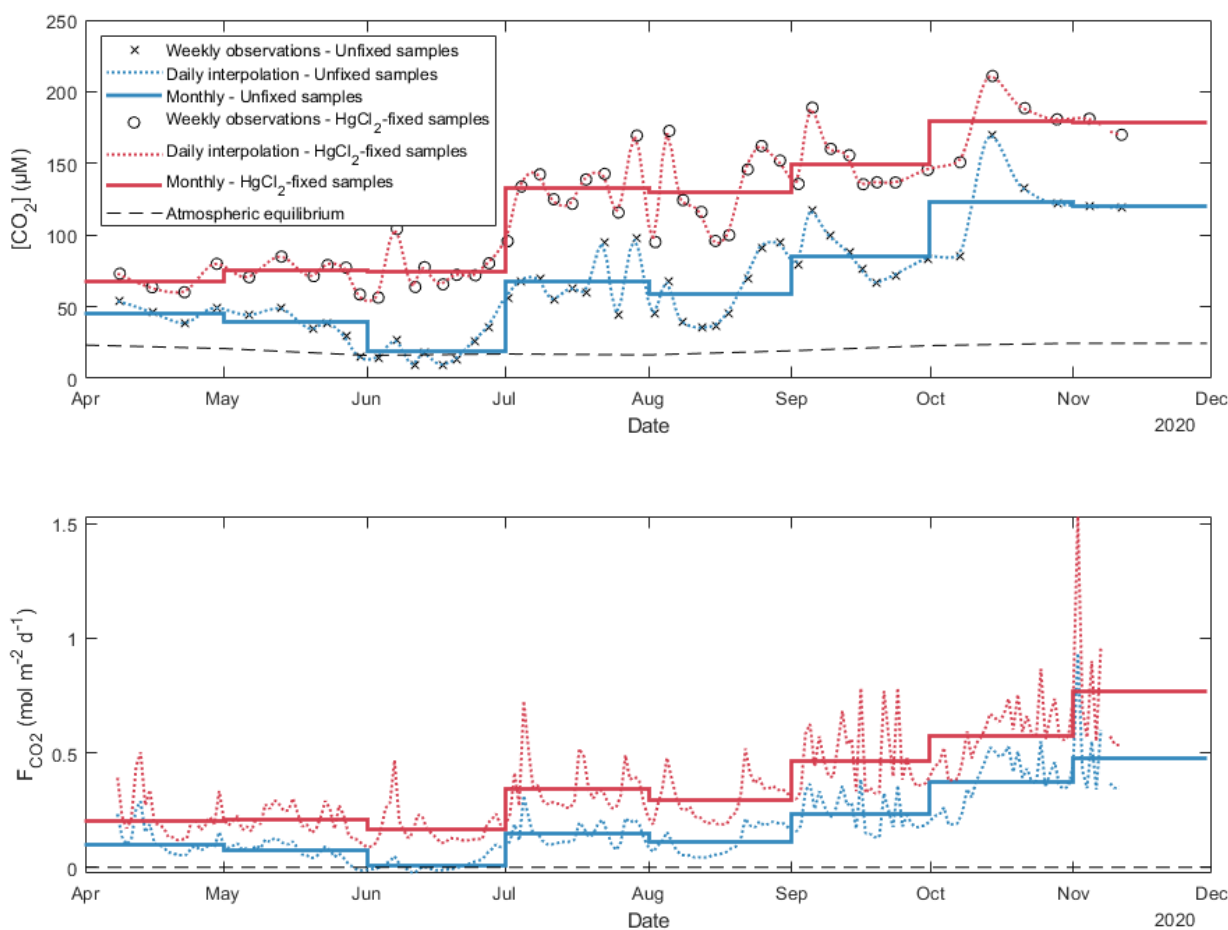
668 In Lake Lundebyvannet, over the ice-free season, average CO<sub>2</sub> concentrations determined following  
669 HgCl<sub>2</sub>-fixation and GC analysis were 82% higher than those obtained from DIC analyses (Tab. 3; Fig.  
670 6 and S3). CO<sub>2</sub> concentrations obtained from HgCl<sub>2</sub>-fixed samples created the illusion that Lake  
671 Lundebyvannet was a steady net source of CO<sub>2</sub> to the atmosphere over the ice-free season with large  
672 CO<sub>2</sub> saturation deficit (Fig. 4) while, in reality, the lake switched from being a net source in May, to a  
673 net sink over a few weeks in June, and returning to a net source in July (Fig. 6 and S3). Indeed,  
674 monthly CO<sub>2</sub> overestimation related to HgCl<sub>2</sub>-fixation reached about 300% in June (Tab. 3).  
675 Propagating this overestimation into the estimates of CO<sub>2</sub> diffusion fluxes with typical wind-based  
676 models yields overestimation of CO<sub>2</sub> fluxes of 108–112% over the ice-free season and up to 2100% in  
677 June (Tab. 3 and S3). Hence, interpreting CO<sub>2</sub> data without correcting for CO<sub>2</sub> overestimation caused  
678 by HgCl<sub>2</sub>-fixation leads to negligence of the role of photosynthesis in lake C cycling with major  
679 implications for current and future predictions of lake CO<sub>2</sub> emissions.

680 The use of HgCl<sub>2</sub> to preserve water samples prior to dissolved gas analyses is part of the current  
681 guidelines for greenhouse gas measurements in freshwater reservoirs (Machado Damazio et al., 2012;  
682 UNESCO/IHA, 2008, 2010). Hence, there is a risk of overestimating CO<sub>2</sub> concentrations and  
683 emissions, in absence of discrete measurement of emissions, from hydropower reservoirs with  
684 consequence on the present and expected greenhouse gas footprint from hydroelectricity. To ensure  
685 precise estimation of greenhouse gas concentration and, possibly, emission from hydropower, the use  
686 of HgCl<sub>2</sub> should therefore be discontinued.

## 687 **5. Conclusion**

688 Mercury is a potent neurotoxin for humans and toxic for the environment and its use should be  
689 discouraged, notably following the Minamata convention on mercury, a global treaty ratified by 126  
690 countries (16 December 2020) to protect human health and the environment from the adverse effects  
691 of mercury. This study further questions the use of HgCl<sub>2</sub> for preservation of poorly buffered (low  
692 ionic strength) water samples with high DOC concentration for analysis of dissolved gases in the  
693 laboratory. Although CuCl<sub>2</sub> is less toxic, it behaved similarly to HgCl<sub>2</sub> and cannot be recommend. In  
694 fact, both chlorinated inhibitors caused a significant decrease in pH shifting the carbonate equilibrium  
695 towards CO<sub>2</sub> and are also suspected to promote carbonate precipitation over long-term storage. The

696 only promising inhibitor tested in this study was AgNO<sub>3</sub> notably for dissolved CO<sub>2</sub>, CH<sub>4</sub> and N<sub>2</sub>O.  
697 Silver nitrate is a suitable substitute for HgCl<sub>2</sub> in low-ionic strength waters, further tests should be  
698 carried out with a range of inhibitor concentration and more diverse water samples. The use of  
699 chemical inhibitors may not be the best approach. Alternatives exist, such as directly measuring gas  
700 concentrations *in situ* with sensors, or sampling the headspace out in the field, and bringing back gas  
701 samples (e.g., Cole et al., 1994; Karlsson et al., 2013; Kling et al., 1991; Valiente et al., 2022), rather  
702 than water samples, to the lab for gas chromatography analyses. However, care must be taken to know  
703 the exact equilibration temperature (Koschorreck et al., 2021) and to avoid gas exchange with the  
704 atmosphere as well as to use a clean background gas during headspace equilibration which can be  
705 challenging in remote environments under harsh meteorological conditions.



706

707 **Fig. 6.** Daily and monthly surface CO<sub>2</sub> concentrations ([CO<sub>2</sub>]; top panel) and diffusion fluxes (F<sub>CO<sub>2</sub></sub>;  
 708 bottom panel) at the water-atmosphere interface from Lake Lundebyvannet (also in Tab. 3). Unfixed  
 709 samples were obtained by DIC analysis. Daily [CO<sub>2</sub>] was interpolated from weekly data using a  
 710 modified spline (see text for details). Diffusion fluxes were calculated following Cole & Caraco  
 711 (1998).

712 We further advise against interpretation of CO<sub>2</sub> concentration data from low ionic strength, circum-  
713 neutral water samples preserved with HgCl<sub>2</sub> or CuCl<sub>2</sub>. The overestimation of CO<sub>2</sub> concentration  
714 caused by HgCl<sub>2</sub> can mask the effect of photosynthesis on lake carbon balance, creating the illusion  
715 that lakes are net CO<sub>2</sub> sources when they are net CO<sub>2</sub> sinks. Our analysis from Lake Lundebyvannet  
716 shows that HgCl<sub>2</sub> fixation led to an overestimation of the CO<sub>2</sub> concentration by a factor of 1.8, on  
717 average, but approaching a factor of 4 during the peak photosynthetic period. An even larger impact is  
718 expected on CO<sub>2</sub> diffusive fluxes which were overestimated by a factor of 2 on average and up to a  
719 factor of >20 during peak photosynthesis. Interpreting such data would have underestimated the  
720 current and future role of aquatic photosynthesis.

#### 721 **Data availability**

722 All data supporting this study will be made available on a permanent repository upon acceptance, e.g.,  
723 Hydroshare.

#### 724 **Author contribution**

725 JET, AK, and TR supervised and PD, KN and FC contributed to the study design. JET, KN and TR  
726 carried out the experiments. PD and TR performed the chemical analyses. JET and FC wrote the first  
727 draft. FC performed the modelling, data, and statistical analyses, and drafted the figures. All co-  
728 authors edited the manuscript.

#### 729 **Competing interests**

730 The contact author has declared that none of the authors has any competing interests.

#### 731 **Acknowledgements**

732 We are grateful to Benoît Demars for research assistance, coordination, and useful comments and  
733 discussions on an earlier version of this manuscript and to Heleen de Wit for discussions. Research  
734 was funded by NIVA and through the Global Change at Northern Latitude (NoLa) project #200033.

735

#### 736 **References**

- 737 Akima, H. (1974). A method of bivariate interpolation and smooth surface fitting based on local  
738 procedures. *Communications of the ACM*, 17(1), 18–20.  
739 <https://doi.org/10.1145/360767.360779>
- 740 Allison, J., Brown, D., & Novo-Gradac, K. (1991). *MINTEQA2/PRODEFA2, a geochemical*  
741 *assessment model for environmental systems: Version 3. 0 user's manual*. GA: US  
742 Environmental Protection Agency.
- 743 Amorim, M. J. B., & Scott-Fordsmand, J. J. (2012). Toxicity of copper nanoparticles and CuCl<sub>2</sub> salt  
744 to *Enchytraeus albidus* worms: Survival, reproduction and avoidance responses.  
745 *Environmental Pollution*, 164, 164–168. <https://doi.org/10.1016/j.envpol.2012.01.015>

- 746 Atekwana, E. A., Molwalefhe, L., Kgaodi, O., & Cruse, A. M. (2016). Effect of evapotranspiration on  
 747 dissolved inorganic carbon and stable carbon isotopic evolution in rivers in semi-arid  
 748 climates: The Okavango Delta in North West Botswana. *Journal of Hydrology: Regional*  
 749 *Studies*, 7, 1–13. <https://doi.org/10.1016/j.ejrh.2016.05.003>
- 750 Borges, A. V., Darchambeau, F., Lambert, T., Morana, C., Allen, G. H., Tambwe, E., Toengaho  
 751 Sembaito, A., Mambo, T., Nlandu Wabakhangazi, J., Descy, J.-P., Teodoru, C. R., &  
 752 Bouillon, S. (2019). Variations in dissolved greenhouse gases (CO<sub>2</sub>, CH<sub>4</sub>, N<sub>2</sub>O) in the Congo  
 753 River network overwhelmingly driven by fluvial-wetland connectivity. *Biogeosciences*,  
 754 16(19), 3801–3834. <https://doi.org/10.5194/bg-16-3801-2019>
- 755 Carroll J.J., Slupsky J.D. & Mather A.E. (1991) The solubility of carbon dioxide in water at low  
 756 pressure. *Journal of Physical and Chemical Reference Data*, 20, 1201-1209.  
 757 <https://doi.org/10.1063/1.555900>
- 758 Chen, C. Y., Driscoll, C., Eagles-Smith, C. A., Eckley, C. S., Gay, D. A., Hsu-Kim, H., Keane, S. E.,  
 759 Kirk, J. L., Mason, R. P., Obrist, D., Selin, H., Selin, N. E., & Thompson, M. R. (2018). A  
 760 Critical Time for Mercury Science to Inform Global Policy. *Environmental Science &*  
 761 *Technology*, 52(17), 9556–9561. <https://doi.org/10.1021/acs.est.8b02286>
- 762 Chen H., Johnston R.C., Mann B.F., Chu R.K., Tolic N., Parks J.M. & Gu B. (2017) Identification of  
 763 mercury and dissolved organic matter complexes using ultrahigh resolution mass  
 764 spectrometry. *Environmental Science & Technology Letters*, 4, 59-65.  
 765 <https://doi.org/10.1021/acs.estlett.6b00460>
- 766 Chou W.C., Gong G.C., Yang C.Y. & Chuang K.Y. (2016) A comparison between field and  
 767 laboratory pH measurements for seawater on the East China Sea shelf. *Limnology and*  
 768 *Oceanography-Methods*, 14, 315-322. <https://doi.org/10.1002/lom3.10091>
- 769 Ciavatta L. & Grimaldi M. (1968) The hydrolysis of mercury(II) chloride, HgCl<sub>2</sub>. *Journal of*  
 770 *Inorganic and Nuclear Chemistry*, 30, 563-581. [https://doi.org/10.1016/0022-1902\(68\)80483-  
 771 X](https://doi.org/10.1016/0022-1902(68)80483-X)
- 772 Clayer, F., Gobeil, C., & Tessier, A. (2016). Rates and pathways of sedimentary organic matter  
 773 mineralization in two basins of a boreal lake: Emphasis on methanogenesis and  
 774 methanotrophy: Methane cycling in boreal lake sediments. *Limnology and Oceanography*,  
 775 61(S1), Article S1. <https://doi.org/10.1002/lno.10323>
- 776 Clayer, F., Thrane, J.-E., Brandt, U., Dörsch, P., & de Wit, H. A. (2021). Boreal Headwater  
 777 Catchment as Hot Spot of Carbon Processing From Headwater to Fjord. *Journal of*  
 778 *Geophysical Research: Biogeosciences*, 126(12), e2021JG006359.  
 779 <https://doi.org/10.1029/2021JG006359>
- 780 Cole, J. J., Caraco, N. F., Kling, G. W., & Kratz, T. K. (1994). Carbon Dioxide Supersaturation in the  
 781 Surface Waters of Lakes. *Science*, 265(5178), Article 5178.  
 782 <https://doi.org/10.1126/science.265.5178.1568>
- 783 Cole, J. J., & Caraco, N. F. (1998). Atmospheric exchange of carbon dioxide in a low-wind  
 784 oligotrophic lake measured by the addition of SF<sub>6</sub>. *Limnology and Oceanography*, 43(4),  
 785 Article 4. <https://doi.org/10.4319/lo.1998.43.4.0647>
- 786 Crusius, J., & Wanninkhof, R. (2003). Gas transfer velocities measured at low wind speed over a lake.  
 787 *Limnology and Oceanography*, 48(3), Article 3. <https://doi.org/10.4319/lo.2003.48.3.1010>
- 788 Deheyn, D. D., Bencheikh-Latmani, R., & Latz, M. I. (2004). Chemical speciation and toxicity of  
 789 metals assessed by three bioluminescence-based assays using marine organisms.  
 790 *Environmental Toxicology*, 19(3), 161–178. <https://doi.org/10.1002/tox.20009>
- 791 de Wit, H. A., Garmo, Ø. A., Jackson-Blake, L. A., Clayer, F., Vogt, R. D., Austnes, K., Kaste, Ø.,  
 792 Gundersen, C. B., Guerrero, J. L., & Hindar, A. (2023). Changing Water Chemistry in One  
 793 Thousand Norwegian Lakes During Three Decades of Cleaner Air and Climate Change.  
 794 *Global Biogeochemical Cycles*, 37(2), e2022GB007509.  
 795 <https://doi.org/10.1029/2022GB007509>
- 796 Dickson A.G., Sabine C.L. & Christian J.R. (2007) *Guide to best practices for ocean CO<sub>2</sub>*  
 797 *measurements*, North Pacific Marine Science Organization.
- 798 Duan, Z., & Mao, S. (2006). A thermodynamic model for calculating methane solubility, density and  
 799 gas phase composition of methane-bearing aqueous fluids from 273 to 523K and from 1 to

- 2000bar. *Geochimica et Cosmochimica Acta*, 70(13), Article 13.  
<https://doi.org/10.1016/j.gca.2006.03.018>
- 802 Foti C., Giuffrè O., Lando G. & Sammartano S. (2009) Interaction of inorganic mercury (II) with  
 803 polyamines, polycarboxylates, and amino acids. *Journal of Chemical & Engineering Data*,  
 804 **54**, 893-903. <https://doi.org/10.1021/jc800685c>
- 805 *Frost API*. (2022). <https://frost.met.no/index.html>
- 806 Golub, M., Desai, A. R., McKinley, G. A., Remucal, C. K., & Stanley, E. H. (2017). Large  
 807 Uncertainty in Estimating pCO<sub>2</sub> From Carbonate Equilibria in Lakes. *Journal of Geophysical*  
 808 *Research: Biogeosciences*, 122(11), 2909–2924. <https://doi.org/10.1002/2017JG003794>
- 809 Guérin, F., Abril, G., Richard, S., Burban, B., Reynouard, C., Seyler, P., & Delmas, R. (2006).  
 810 Methane and carbon dioxide emissions from tropical reservoirs: Significance of downstream  
 811 rivers. *Geophysical Research Letters*, 33(21). <https://doi.org/10.1029/2006GL027929>
- 812 Guérin, F., Abril, G., Serça, D., Delon, C., Richard, S., Delmas, R., Tremblay, A., & Varfalvy, L.  
 813 (2007). Gas transfer velocities of CO<sub>2</sub> and CH<sub>4</sub> in a tropical reservoir and its river  
 814 downstream. *Journal of Marine Systems*, 66(1), Article 1.  
 815 <https://doi.org/10.1016/j.jmarsys.2006.03.019>
- 816 Halmi, M. I. E., Kassim, A., & Shukor, M. Y. (2019). Assessment of heavy metal toxicity using a  
 817 luminescent bacterial test based on *Photobacterium* sp. Strain MIE. *Rendiconti Lincei. Scienze*  
 818 *Fisiche e Naturali*, 30(3), 589–601. <https://doi.org/10.1007/s12210-019-00809-5>
- 819 Hagman, C. H. C., Ballot, A., Hjermand, D. Ø., Skjelbred, B., Brettum, P., & Ptacnik, R. (2015). The  
 820 occurrence and spread of *Gonyostomum semen* (Ehr.) Diesing (Raphidophyceae) in  
 821 Norwegian lakes. *Hydrobiologia*, 744(1), 1–14. <https://doi.org/10.1007/s10750-014-2050-y>
- 822 Hamme R.C. & Emerson S.R. (2004) The solubility of neon, nitrogen and argon in distilled water and  
 823 seawater. *Deep-Sea Research Part I-Oceanographic Research Papers*, **51**, 1517-1528.  
 824 <https://doi.org/10.1016/j.dsr.2004.06.009>
- 825 Hassen A., Saidi N., Cherif M. & Boudabous A. (1998) Resistance of environmental bacteria to heavy  
 826 metals. *Bioresource technology*, **64**, 7-15. [https://doi.org/10.1016/S0960-8524\(97\)00161-2](https://doi.org/10.1016/S0960-8524(97)00161-2)
- 827 Hessen, D. O., Håll, J. P., Thrane, J.-E., & Andersen, T. (2017). Coupling dissolved organic carbon,  
 828 CO<sub>2</sub> and productivity in boreal lakes. *Freshwater Biology*, 62(5), 945–953.  
 829 <https://doi.org/10.1111/fwb.12914>
- 830 Hilgert, S., Scapulatempo Fernandes, C. V., & Fuchs, S. (2019). Redistribution of methane emission  
 831 hot spots under drawdown conditions. *Science of The Total Environment*, 646, 958–971.  
 832 <https://doi.org/10.1016/j.scitotenv.2018.07.338>
- 833 Horvatić J. & Peršić V. (2007) The effect of Ni<sup>2+</sup>, Co<sup>2+</sup>, Zn<sup>2+</sup>, Cd<sup>2+</sup> and Hg<sup>2+</sup> on the growth  
 834 rate of marine diatom *Phaeodactylum tricornutum* Bohlin: microplate growth inhibition test.  
 835 *Bulletin of Environmental Contamination and Toxicology*, **79**, 494-498.  
 836 <https://doi.org/10.1007/s00128-007-9291-7>
- 837 Houle, D., Augustin, F., & Couture, S. (2022). Rapid improvement of lake acid–base status in  
 838 Atlantic Canada following steep decline in precipitation acidity. *Canadian Journal of*  
 839 *Fisheries and Aquatic Sciences*, 79(12), 2126–2137. <https://doi.org/10.1139/cjfas-2021-0349>
- 840 IEA. (2020). *Key World Energy Statistics 2020*. IEA, International Energy Agency.  
 841 <https://www.iea.org/reports/key-world-energy-statistics-2020>
- 842 Jeffrey, L. C., Santos, I. R., Tait, D. R., Makings, U., & Maher, D. T. (2018). Seasonal Drivers of  
 843 Carbon Dioxide Dynamics in a Hydrologically Modified Subtropical Tidal River and Estuary  
 844 (Caboolture River, Australia). *Journal of Geophysical Research: Biogeosciences*, 123(6),  
 845 1827–1849. <https://doi.org/10.1029/2017JG004023>
- 846 Jonsson, A., Meili, M., Bergström, A.-K., & Jansson, M. (2001). Whole-lake mineralization of  
 847 allochthonous and autochthonous organic carbon in a large humic lake (örträsket, N.  
 848 Sweden). *Limnology and Oceanography*, 46(7), 1691–1700.  
 849 <https://doi.org/10.4319/lo.2001.46.7.1691>
- 850 Karlsson, J., Giesler, R., Persson, J., & Lundin, E. (2013). High emission of carbon dioxide and  
 851 methane during ice thaw in high latitude lakes. *Geophysical Research Letters*, 40(6), Article  
 852 6. <https://doi.org/10.1002/grl.50152>

- 853 Khwaja, A. R., Bloom, P. R., & Brezonik, P. L. (2006). Binding Constants of Divalent Mercury  
854 (Hg<sub>2</sub><sup>+</sup>) in Soil Humic Acids and Soil Organic Matter. *Environmental Science & Technology*,  
855 40(3), 844–849. <https://doi.org/10.1021/es051085c>
- 856 Kim, D., Mahabadi, N., Jang, J., & van Paassen, L. A. (2020). Assessing the Kinetics and Pore-Scale  
857 Characteristics of Biological Calcium Carbonate Precipitation in Porous Media using a  
858 Microfluidic Chip Experiment. *Water Resources Research*, 56(2), e2019WR025420.  
859 <https://doi.org/10.1029/2019WR025420>
- 860 Klaus, M. (2023). Decadal increase in groundwater inorganic carbon concentrations across Sweden.  
861 *Communications Earth & Environment*, 4(1), Article 1. [https://doi.org/10.1038/s43247-023-](https://doi.org/10.1038/s43247-023-00885-4)  
862 00885-4
- 863 Kling, G. W., Kipphut, G. W., & Miller, M. C. (1991). Arctic Lakes and Streams as Gas Conduits to  
864 the Atmosphere: Implications for Tundra Carbon Budgets. *Science*, 251(4991), 298–301.  
865 <https://doi.org/10.1126/science.251.4991.298>
- 866 Knowles, R. (1982). Denitrification. *Microbiological Reviews*, 46(1), 43–70.  
867 <https://doi.org/10.1128/mr.46.1.43-70.1982>
- 868 Kokic, J., Wallin, M. B., Chmiel, H. E., Denfeld, B. A., & Sobek, S. (2015). Carbon dioxide evasion  
869 from headwater systems strongly contributes to the total export of carbon from a small boreal  
870 lake catchment. *Journal of Geophysical Research: Biogeosciences*, 120(1), 13–28.  
871 <https://doi.org/10.1002/2014JG002706>
- 872 Koschorreck, M., Prairie, Y. T., Kim, J., & Marcé, R. (2021). Technical note: CO<sub>2</sub> is not like CH<sub>4</sub> –  
873 limits of and corrections to the headspace method to analyse pCO<sub>2</sub> in fresh water.  
874 *Biogeosciences*, 18(5), 1619–1627. <https://doi.org/10.5194/bg-18-1619-2021>
- 875 Larrañaga, M., Lewis, R., & Lewis, R. (2016). Hawley’s Condensed Chemical Dictionary, Sixteenth  
876 Edition. i–xiii. <https://doi.org/10.1002/9781119312468.fmatter>
- 877 Liang X., Lu X., Zhao J., Liang L., Zeng E.Y. & Gu B. (2019) Stepwise reduction approach reveals  
878 mercury competitive binding and exchange reactions within natural organic matter and mixed  
879 organic ligands. *Environmental Science & Technology*, 53, 10685-10694.  
880 <https://doi.org/10.1021/acs.est.9b02586>
- 881 Machado Damazio, J., Cordeiro Geber de Melo, A., Piñeiro Maceira, M. E., Medeiros, A., Negrini,  
882 M., Alm, J., Schei, T. A., Tateda, Y., Smith, B., & Nielsen, N. (2012). *Guidelines for*  
883 *quantitative analysis of net GHG emissions from reservoirs: Volume 1: Measurement*  
884 *Programmes and Data Analysis*. International Energy Agency (IEA).  
885 [https://www.ieahydro.org/media/992f6848/GHG\\_Guidelines\\_22October2012\\_Final.pdf](https://www.ieahydro.org/media/992f6848/GHG_Guidelines_22October2012_Final.pdf)
- 886 Magen, C., Lapham, L. L., Pohlman, J. W., Marshall, K., Bosman, S., Casso, M., & Chanton, J. P.  
887 (2014). A simple headspace equilibration method for measuring dissolved methane.  
888 *Limnology and Oceanography: Methods*, 12(9), 637–650.  
889 <https://doi.org/10.4319/lom.2014.12.637>
- 890 Miller, C. L., Southworth, G., Brooks, S., Liang, L., & Gu, B. (2009). Kinetic Controls on the  
891 Complexation between Mercury and Dissolved Organic Matter in a Contaminated  
892 Environment. *Environmental Science & Technology*, 43(22), 8548–8553.  
893 <https://doi.org/10.1021/es901891t>
- 894 Millero F.J., Huang F. & Laferiere A.L. (2002) Solubility of oxygen in the major sea salts as a  
895 function of concentration and temperature. *Marine Chemistry*, 78, 217-230.  
896 [https://doi.org/10.1016/S0304-4203\(02\)00034-8](https://doi.org/10.1016/S0304-4203(02)00034-8)
- 897 Myrstener, M., Fork, M. L., Bergström, A.-K., Puts, I. C., Hauptmann, D., Isles, P. D. F., Burrows, R.  
898 M., & Sponseller, R. A. (2022). Resolving the Drivers of Algal Nutrient Limitation from  
899 Boreal to Arctic Lakes and Streams. *Ecosystems*, 25(8), 1682–1699.  
900 <https://doi.org/10.1007/s10021-022-00759-4>
- 901 Mørkved, P. T., Dörsch, P., & Bakken, L. R. (2007). The N<sub>2</sub>O product ratio of nitrification and its  
902 dependence on long-term changes in soil pH. *Soil Biology and Biochemistry*, 39(8), 2048–  
903 2057. <https://doi.org/10.1016/j.soilbio.2007.03.006>
- 904 NILU. (2022). *EBAS*. <https://ebas-data.nilu.no/Default.aspx>
- 905 Nowack, B., Krug, H. F., & Height, M. (2011). 120 Years of Nanosilver History: Implications for  
906 Policy Makers. *Environmental Science & Technology*, 45(4), 1177–1183.  
907 <https://doi.org/10.1021/es103316q>



- 908 NPIRS. (2023). *Purdue University*. <https://www.npirs.org/public>
- 909 Okuku, E. O., Bouillon, S., Tole, M., & Borges, A. V. (2019). Diffusive emissions of methane and  
910 nitrous oxide from a cascade of tropical hydropower reservoirs in Kenya. *Lakes &*  
911 *Reservoirs: Science, Policy and Management for Sustainable Use*, 24(2), 127–135.  
912 <https://doi.org/10.1111/lre.12264>
- 913 Parkhurst, D. L., & Appelo, C. A. J. (2013). *Description of input and examples for PHREEQC version*  
914 *3—A computer program for speciation, batch-reaction, one-dimensional transport, and*  
915 *inverse geochemical calculations: U.S. Geological Survey Techniques and Methods* (book 6,  
916 chap. A43; p. 497). USGS. <http://pubs.usgs.gov/tm/06/a43/>
- 917 Powell K.J., Brown P.L., Byrne R.H., Gajda T., Hefter G., Sjöberg S. & Wanner H. (2004) Chemical  
918 speciation of Hg (II) with environmental inorganic ligands. *Australian Journal of Chemistry*,  
919 **57**, 993-1000. <https://doi.org/10.1071/CH04063>
- 920 Rai L.C., Gaur J.P. & Kumar H.D. (1981) Phycology and heavy-metal pollution. *Biological Reviews*,  
921 **56**, 99-151. <https://doi.org/10.1111/j.1469-185X.1981.tb00345.x>
- 922 Ratte, H. T. (1999). Bioaccumulation and toxicity of silver compounds: A review. *Environmental*  
923 *Toxicology and Chemistry*, 18(1), 89–108. <https://doi.org/10.1002/etc.5620180112>
- 924 Ray, R., Miyajima, T., Watanabe, A., Yoshikai, M., Ferrera, C. M., Orizar, I., Nakamura, T., San  
925 Diego-McGlone, M. L., Herrera, E. C., & Nadaoka, K. (2021). Dissolved and particulate  
926 carbon export from a tropical mangrove-dominated riverine system. *Limnology and*  
927 *Oceanography*, 66(11), 3944–3962. <https://doi.org/10.1002/lno.11934>
- 928 Rees, A. P., Brown, I. J., Jayakumar, A., Lessin, G., Somerfield, P. J., & Ward, B. B. (2021).  
929 Biological nitrous oxide consumption in oxygenated waters of the high latitude Atlantic  
930 Ocean. *Communications Earth & Environment*, 2(1), Article 1.  
931 <https://doi.org/10.1038/s43247-021-00104-y>
- 932 Rippner, D. A., Margenot, A. J., Fakra, S. C., Aguilera, L. A., Li, C., Sohng, J., Dynarski, K. A.,  
933 Waterhouse, H., McElroy, N., Wade, J., Hind, S. R., Green, P. G., Peak, D., McElrone, A. J.,  
934 Chen, N., Feng, R., Scow, K. M., & Parikh, S. J. (2021). Microbial response to copper oxide  
935 nanoparticles in soils is controlled by land use rather than copper fate. *Environmental*  
936 *Science: Nano*, 8(12), 3560–3576. <https://doi.org/10.1039/D1EN00656H>
- 937 Rohrlack T., Frostad P., Riise G. & Hagman C.H.C. (2020) Motile phytoplankton species such as  
938 *Gonyostomum semen* can significantly reduce CO<sub>2</sub> emissions from boreal lakes.  
939 *Limnologica*, **84**, 125810. <https://doi.org/10.1016/j.limno.2020.125810>
- 940 Schubert, C. J., Diem, T., & Eugster, W. (2012). Methane Emissions from a Small Wind Shielded  
941 Lake Determined by Eddy Covariance, Flux Chambers, Anchored Funnels, and Boundary  
942 Model Calculations: A Comparison. *Environmental Science & Technology*, 46(8), 4515–  
943 4522. <https://doi.org/10.1021/es203465x>
- 944 Seitzinger, S. P. (1988). Denitrification in freshwater and coastal marine ecosystems: Ecological and  
945 geochemical significance. *Limnology and Oceanography*, 33(4part2), 702–724.  
946 <https://doi.org/10.4319/lo.1988.33.4part2.0702>
- 947 Silver S. & Phung L.T. (2005) A bacterial view of the periodic table: genes and proteins for toxic  
948 inorganic ions. *Journal of Industrial Microbiology & Biotechnology*, **32**, 587-605.  
949 <https://doi.org/10.1007/s10295-005-0019-6>
- 950 Skjelkvåle, B. L., & de Wit, H. A. (2011). Trends in precipitation chemistry, surface water chemistry  
951 and aquatic biota in acidified areas in Europe and North America from 1990 to 2008 (ICP  
952 Waters report 106/2011). In 126. Norsk institutt for vannforskning.  
953 <https://niva.brage.unit.no/niva-xmlui/handle/11250/215591>
- 954 Skjellberg, U. (2008). Competition among thiols and inorganic sulfides and polysulfides for Hg and  
955 MeHg in wetland soils and sediments under suboxic conditions: Illumination of controversies  
956 and implications for MeHg net production. *Journal of Geophysical Research:*  
957 *Biogeosciences*, 113(G2). <https://doi.org/10.1029/2008JG000745>
- 958 Sobek, S., Algesten, G., Bergström, A.-K., Jansson, M., & Tranvik, L. J. (2003). The catchment and  
959 climate regulation of pCO<sub>2</sub> in boreal lakes. *Global Change Biology*, 9(4), 630–641.  
960 <https://doi.org/10.1046/j.1365-2486.2003.00619.x>
- 961 Stumm W. & Morgan J.J. (1981) *Aquatic Chemistry. An introduction emphasizing chemical*  
962 *equilibria in natural waters*, Wiley Interscience, New York.

- 963 Stumm, W., & Morgan, J. J. (1996). *Aquatic chemistry: Chemical equilibria and rates in natural*  
 964 *waters* (3rd ed.). Wiley.
- 965 Taipale S.J. & Sonninen E. (2009) The influence of preservation method and time on the delta C-13  
 966 value of dissolved inorganic carbon in water samples. *Rapid Communications in Mass*  
 967 *Spectrometry*, **23**, 2507-2510. <https://doi.org/10.1002/rcm.4072>
- 968 Takahashi H.A., Handa H., Sugiyama A., Matsushita M., Kondo M., Kimura H. & Tsujimura M.  
 969 (2019) Filtration and exposure to benzalkonium chloride or sodium chloride to preserve water  
 970 samples for dissolved inorganic carbon analysis. *Geochemical Journal*, **53**, 305-318.  
 971 <https://doi.org/10.2343/geochemj.2.0570>
- 972 Thottathil, S. D., Reis, P. C. J., & Prairie, Y. T. (2019). Methane oxidation kinetics in northern  
 973 freshwater lakes. *Biogeochemistry*, *143*(1), Article 1. [https://doi.org/10.1007/s10533-019-](https://doi.org/10.1007/s10533-019-00552-x)  
 974 [00552-x](https://doi.org/10.1007/s10533-019-00552-x)
- 975 Tipping E. (2007) Modelling the interactions of Hg(II) and methylmercury with humic substances  
 976 using WHAM/Model VI. *Applied Geochemistry*, **22**, 1624-1635.
- 977 Tørseth, K., Aas, W., Breivik, K., Fjæraa, A. M., Fiebig, M., Hjellbrekke, A. G., Lund Myhre, C.,  
 978 Solberg, S., & Yttri, K. E. (2012). Introduction to the European Monitoring and Evaluation  
 979 Programme (EMEP) and observed atmospheric composition change during  
 980 1972–2009. *Atmospheric Chemistry and Physics*, *12*(12), 5447–5481.  
 981 <https://doi.org/10.5194/acp-12-5447-2012>
- 982 Ullmann, F., Gerhartz, W., Yamamoto, Y. S., Campbell, F. T., Pfefferkorn, R., & Rounsaville, J. F.  
 983 (1985). Ullmann's encyclopedia of industrial chemistry (5th, completely rev. ed ed.). VCH.
- 984 UNESCO/IHA. (2008). *Assessment of the GHG status of freshwater reservoirs: Scoping paper*  
 985 (IHP/GHG-WG/3; p. 28). UNESCO/IHA, International Hydropower Association -  
 986 International Hydrological Programme, Working Group on Greenhouse Gas Status of  
 987 Freshwater Reservoirs. <https://unesdoc.unesco.org/ark:/48223/pf0000181713>
- 988 UNESCO/IHA. (2010). *GHG Measurement Guidelines for Freshwater Reservoirs* (p. 154).  
 989 UNESCO/IHA, International Hydropower Association.  
 990 [https://www.hydropower.org/publications/ghg-measurement-guidelines-for-freshwater-](https://www.hydropower.org/publications/ghg-measurement-guidelines-for-freshwater-reservoirs)  
 991 [reservoirs](https://www.hydropower.org/publications/ghg-measurement-guidelines-for-freshwater-reservoirs)
- 992 Urabe, J., Iwata, T., Yagami, Y., Kato, E., Suzuki, T., Hino, S., & Ban, S. (2011). Within-lake and  
 993 watershed determinants of carbon dioxide in surface water: A comparative analysis of a  
 994 variety of lakes in the Japanese Islands. *Limnology and Oceanography*, *56*(1), 49–60.  
 995 <https://doi.org/10.4319/lo.2011.56.1.0049>
- 996 Vachon, D., & Prairie, Y. T. (2013). The ecosystem size and shape dependence of gas transfer  
 997 velocity versus wind speed relationships in lakes. *Canadian Journal of Fisheries and Aquatic*  
 998 *Sciences*, *70*(12), Article 12. <https://doi.org/10.1139/cjfas-2013-0241>
- 999 Valiente, N., Eiler, A., Alleesson, L., Andersen, T., Clayer, F., Crapart, C., Dörsch, P., Fontaine, L.,  
 1000 Heuschele, J., Vogt, R., Wei, J., de Wit, H. A., & Hessen, D. O. (2022). *Catchment properties*  
 1001 *as predictors of greenhouse gas concentrations across a gradient of boreal lakes*.  
 1002 *10*(880619). <https://doi.org/10.3389/fenvs.2022.880619>
- 1003 Valinia, S., Englund, G., Moldan, F., Futter, M. N., Köhler, S. J., Bishop, K., & Fölster, J. (2014).  
 1004 Assessing anthropogenic impact on boreal lakes with historical fish species distribution data  
 1005 and hydrogeochemical modeling. *Global Change Biology*, *20*(9), 2752–2764.  
 1006 <https://doi.org/10.1111/gcb.12527>
- 1007 van Grinsven, S., Oswald, K., Wehrli, B., Jegge, C., Zopfi, J., Lehmann, M. F., & Schubert, C. J.  
 1008 (2021). Methane oxidation in the waters of a humic-rich boreal lake stimulated by  
 1009 photosynthesis, nitrite, Fe(III) and humics. *Biogeochemistry*, *18*(10), 3087–3101.  
 1010 <https://doi.org/10.5194/bg-18-3087-2021>
- 1011 Wanninkhof, R. (2014). Relationship between wind speed and gas exchange over the ocean revisited.  
 1012 *Limnology and Oceanography: Methods*, *12*(6), Article 6.  
 1013 <https://doi.org/10.4319/lom.2014.12.351>
- 1014 Webb, J. R., Santos, I. R., Maher, D. T., Macdonald, B., Robson, B., Isaac, P., & McHugh, I. (2018).  
 1015 Terrestrial versus aquatic carbon fluxes in a subtropical agricultural floodplain over an annual  
 1016 cycle. *Agricultural and Forest Meteorology*, *260–261*, 262–272.  
 1017 <https://doi.org/10.1016/j.agrformet.2018.06.015>

- 1018 Weiss R.F. & Price B.A. (1980) Nitrous oxide solubility in water and seawater. *Marine Chemistry*, **8**,  
1019 347-359. [https://doi.org/10.1016/0304-4203\(80\)90024-9](https://doi.org/10.1016/0304-4203(80)90024-9)
- 1020 Weyhenmeyer, G. A., Hartmann, J., Hessen, D. O., Kopáček, J., Hejzlar, J., Jacquet, S., Hamilton, S.  
1021 K., Verburg, P., Leach, T. H., Schmid, M., Flaim, G., Nöges, T., Nöges, P., Wentzky, V. C.,  
1022 Rogora, M., Rusak, J. A., Kosten, S., Paterson, A. M., Teubner, K., ... Zechmeister, T.  
1023 (2019). Widespread diminishing anthropogenic effects on calcium in freshwaters. *Scientific*  
1024 *Reports*, *9*(1), Article 1. <https://doi.org/10.1038/s41598-019-46838-w>
- 1025 Wilhelm E., Battino R. & Wilcock R.J. (1977) Low-pressure solubility of gases in liquid water.  
1026 *Chemical Reviews*, **77**, 219-262. <https://doi.org/10.1021/cr60306a003>
- 1027 Wilson J., Munizzi J. & Erhardt A.M. (2020) Preservation methods for the isotopic composition of  
1028 dissolved carbon species in non-ideal conditions. *Rapid Communications in Mass*  
1029 *Spectrometry*, **34**. <https://doi.org/10.1002/rcm.8903>
- 1030 Xiao, S., Yang, H., Liu, D., Zhang, C., Lei, D., Wang, Y., Peng, F., Li, Y., Wang, C., Li, X., Wu, G.,  
1031 & Liu, L. (2014). Gas transfer velocities of methane and carbon dioxide in a subtropical  
1032 shallow pond. *Tellus B: Chemical and Physical Meteorology*, *66*(1), 23795.  
1033 <https://doi.org/10.3402/tellusb.v66.23795>
- 1034 Xu F.F. & Imlay J.A. (2012) Silver(I), Mercury(II), Cadmium(II), and Zinc(II) Target Exposed  
1035 Enzymic Iron-Sulfur Clusters when They Toxicify Escherichia coli. *Applied and Environmental*  
1036 *Microbiology*, **78**, 3614-3621. <https://doi.org/10.1128/aem.07368-11>
- 1037 Yamamoto S., Alcauskas J.B. & Crozier T.E. (1976) Solubility of methane in distilled water and  
1038 seawater. *Journal of Chemical and Engineering Data*, **21**, 78-80.  
1039 <https://doi.org/10.1021/jc60068a029>
- 1040 Yan, F., Sillanpää, M., Kang, S., Aho, K. S., Qu, B., Wei, D., Li, X., Li, C., & Raymond, P. A.  
1041 (2018). Lakes on the Tibetan Plateau as Conduits of Greenhouse Gases to the Atmosphere.  
1042 *Journal of Geophysical Research: Biogeosciences*, *123*(7), 2091–2103.  
1043 <https://doi.org/10.1029/2017JG004379>
- 1044 Yang H., Andersen T., Dorsch P., Tominaga K., Thrane J.E. & Hessen D.O. (2015) Greenhouse gas  
1045 metabolism in Nordic boreal lakes. *Biogeochemistry*, **126**, 211-225.  
1046 <https://doi.org/10.1007/s10533-015-0154-8>
- 1047